HYBRID DWT-DCT ALGORITHM FOR IMAGE AND VIDEO COMPRESSION APPLICATIONS

A Thesis

Submitted to the College of Graduate Studies and Research

In Partial Fulfillment of the Requirements

For the Degree of Master of Science

In the Department of Electrical and Computer Engineering

University of Saskatchewan

Saskatoon, Saskatchewan, Canada

By

Suchitra Shrestha

PERMISSION TO USE

I agree that the Library, University of Saskatchewan, may make this thesis freely available for inspection. I further agree that permission for copying of this thesis for scholarly purposes may be granted to the professors who supervised the thesis work recorded herein or, in their absence, by the Head of the Department of Electrical and Computer Engineering or the Dean of the College of Engineering. It is understood that due recognition will be given to me and to the University of Saskatchewan in any use of the material in this thesis. Copying or publication or any other use of this thesis for financial gain without approval by the University of Saskatchewan and my written permission is prohibited.

Requests for permission to copy or to make other use of material in this thesis in whole or part should be addressed to:

Head of the Department of Electrical and Computer Engineering

57 Campus Drive

University of Saskatchewan

Saskatoon, SK

Canada, S7N 5A9

ABSTRACT

Digital image and video in their raw form require an enormous amount of storage capacity. Considering the important role played by digital imaging and video, it is necessary to develop a system that produces high degree of compression while preserving critical image/video information. There are various transformation techniques used for data compression. Discrete Cosine Transform (DCT) and Discrete Wavelet Transform (DWT) are the most commonly used transformation. DCT has high energy compaction property and requires less computational resources. On the other hand, DWT is multiresolution transformation.

In this work, we propose a hybrid DWT-DCT algorithm for image compression and reconstruction taking benefit from the advantages of both algorithms. The algorithm performs the Discrete Cosine Transform (DCT) on the Discrete Wavelet Transform (DWT) coefficients. Simulations have been conducted on several natural, benchmark, medical and endoscopic images. Several QCIF, high definition, and endoscopic videos have also been used to demonstrate the advantage of the proposed scheme.

The simulation results show that the proposed hybrid DWT-DCT algorithm performs much better than the standalone JPEG-based DCT, DWT, and WHT algorithms in terms of peak signal to noise ratio (*PSNR*), as well as visual perception at higher compression ratio. The new scheme reduces “false contouring” and “blocking artifacts” significantly. The rate distortion analysis shows that for a fixed level of distortion, the number of bits required to transmit the hybrid coefficients would be less than those required for other schemes Furthermore, the proposed algorithm is also compared with the some existing hybrid algorithms. The comparison results show that, the proposed hybrid algorithm has better performance and reconstruction quality. The proposed scheme is intended to be used as the image/video compressor engine in imaging and video applications.

ACKNOWLEDGMENTS

The work presented in this thesis has been carried out at Department of Electrical and Computer Engineering, University of Saskatchewan, Saskatoon, Saskatchewan during the years 2008 - 2010 under kind supervision of Professor Dr. Khan Wahid.

First I would like to express my deepest gratitude to my advisor Professor Dr. Khan Wahid for encouraging me to work on this topic in this thesis. Beside his broad knowledge, his mind provoking questions, and the thoughtful discussions have been a valuable source, inspiration, and motivation throughout my study, and also the way for completion for this thesis.

I express my gratitude to Department of Electrical and Computer Engineering, University of Saskatchewan. I would also like to express my appreciation to all the professors of Department of Electrical and Computer Engineering, for their course supervision. I greatly appreciate, and would like to thank Ms Darla for taking excellent care of our administrative needs.

The journey towards my study would not have been full of fun and enjoyment without friendship and assistance from my colleagues. I extend my thanks to my colleague for giving me friendly environment and endless support.

Last but not least, my warmest gratitude goes to my husband Mr. Dipendra Rai, my parents Mr. Jib Lal Shrestha and Mrs. Krishna Shrestha, and my sisters. Their endless love, encouragement, support had played a great role in fulfilling my dreams and bringing this work to completion. I would like to dedicate this thesis to them.

-Suchitra Shrestha

TABLE OF CONTENTS

LIST OF TABLES

LIST OF FIGURES

ABBREVIATIONS AND SYMBOLS

1-D	One Dimensional
2-D	Two Dimensional
bpp	Bits Per Pixel
CR	Compression Ratio
CT	Computed Tomography
dB	Decibel
DCT	Discrete Cosine Transform
DFT	Discrete Fourier Transform
DST	Discrete Cosine Transform
DWHT	Discrete Walsh Hadamard Transform
DWT	Discrete Wavelet Transform
EZW	Embedded Zero tree Wavelet
FFT	Fast Fourier Transform
HD	High Definition
HH	High High
HL	High Low
HPF	High Pass Filter
JPEG	Joint Photographic Expert Group
KLT	Karhunen-Loeve Transform
LH	Low High
LL	Low Low
LPF	Low Pass Filter
MSE	Mean Square Error
PSNR	Peak Signal to Noise Ratio
QCIF	Quarterly Common Intermediate Format
Q-Table	Quantization Table

R	Correlation Matrix
SF	Scaling Factor
SPECK	Set Partitioning Embedded Block Coder
SPIHT	Set Partitioning In Hierarchical Coding Technique
SSIM	Structural Similarity
TIFF	Tagged Image File Format
US	Ultrasound
WCES	Wireless Capsule Endoscopic System
WHT	Walsh Hadamard Transform
μ	Mean
ρ	Correlation Coefficient
σ	Standard Deviation
σ^2	Variance

LIST OF PUBLICATIONS

This work has resulted in the following conferences and journals publications.

[P1] **Suchitra Shrestha** and Khan Wahid, "Hybrid DWT-DCT Algorithm for Biomedical Image and Video Compression Applications", Proc. of the 10th IEEE International Conference on Information Sciences, Signal Processing and their Applications, pp. 280-283, 2010.

[P2] **Suchitra Shrestha** and Khan A Wahid, "A sub-sample based hybrid DWT-DCT algorithm for medical imaging applications," Cyber Journals: Multidisciplinary Journals in Science and Technology, Nov. 24, 2010.

CHAPTER 1
INTRODUCTION

Study has shown that the 90% of total volume of data in internet access consists of image and video related data [1]. Image and video in their raw (uncompressed) form requires huge storage space. Such raw data needs large transmission bandwidth for the transmission over the network. Hence, lots of researches have been conducted in the field of data compression system. However, in this modern internet age, the demand for data transmission and the data storage are increasing. In this concern, data compression and reconstruction is the only option to relieve the network congestion. The compression technique reduces the size of data, which in turn requires less bandwidth and less transmission time and related cost. There are algorithms developed for the data compression such as: Discrete Cosine Transform (DCT), Discrete Wavelet Transform (DWT), Walsh Hadamard Transform (WHT), etc. These transform techniques are explained in Chapter 2.

1.1 Image

An image is the two dimensional (2-D) picture that gives appearance to a subject usually a physical object or a person. It is digitally represented by a rectangular matrix of dots arranged in rows and columns. Figure 1.1 shows the standard image 'Einstein'. The size of the row (M) and column (N) gives the size (or resolution) of $M \times N$ image. A small block (8×8) of the image is indicated at the lower right corner in the form of matrix. Each element in the matrix represents the dots of the image. Each dot represents the pixel value at that position.

1.2 Redundancy

Data compression is essentially a redundancy reduction technique. It is the process of reducing the amount of data required to represent a given quantity of information. For the transmission of same amount of information, different amount of data might be used. If the same

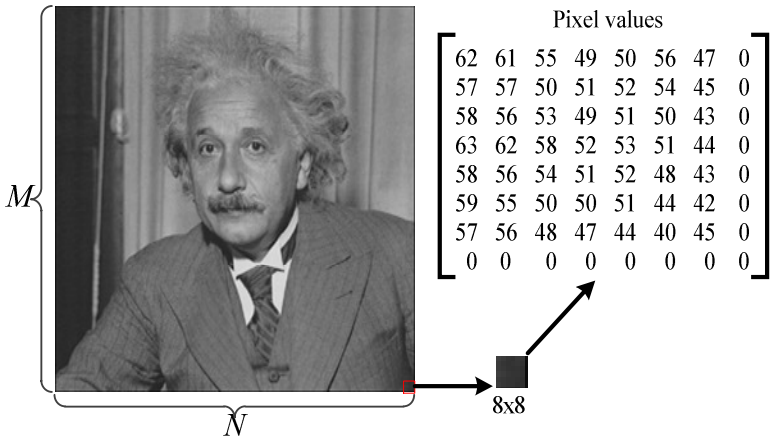

Figure 1.1. Digital representation of an image 'Einstein'[1]

information can be represented using different amounts of data, and, the representations that require more data than actual information, is referred as data redundancy [2]. There are three kinds of redundancies that may present in the image and video.

I. Spatial redundancy

II. Spectral redundancy

III. Temporal redundancy

Spatial Redundancy: Most of the image contains correlated pixels. If the neighbouring pixels are spatially correlated to each other, then it is known as spatial redundancy. In this thesis work, the spatial redundancy has been taken into consideration and data compression algorithm is analysed by reducing the spatial redundancy.

Spectral redundancy: A correlation between different colour planes i.e. spectral bands in an image and video is called spectral redundancy.

Temporal redundancy: In the video sequences, the adjacent frames are generally correlated. This kind of correlation is called the temporal redundancy. An example of temporal redundancy is shown in Figure 1.2. The figure shows the three consecutive frames of a video sequence 'Martin'. It is observed all of the frames are same except the position of hands of the person.

[1] Image source: Internet: http://sipi.usc.edu/database/index.html

Frame 1 Frame 2 Frame 3

Figure 1.2. Frames of a video sequence 'Martin'[2]

1.3 Data Compression

The data redundancies require large storage space. The compression can be achieved by reducing these redundant data is referred as data compression. Mathematically, by data compression means process of transforming pixel array of an image into statistically uncorrelated data set.

1.3.1 Necessity of data compression

Example 1.1: Importance of data compression

A full motion colour video of size 640×480 has 8 bits per pixel. If it is 1 minute long, and has 30 frames per second. The total storage required for this video is

$$Storage = \frac{\overbrace{640 \times 480}^{\text{resolution}} \times \overbrace{3 \times 8}^{\text{RGB bits}} \times \overbrace{60}^{\text{seconds}} \times \overbrace{30}^{\text{frames}}}{\underbrace{8}_{\text{bits}}} bytes$$

$$= 1.66 \text{ GB (bytes)}$$

This is very huge in size. When the video is intended to transmit through cable Modem having 5 Mbps then, the time required to transmit this video is calculated as:

$$Transmission\ time = \frac{1.66 \times 10^9 \times 8}{5 \times 10^6 \times 60}$$

$$= 44\ minutes$$

Example 1.1 clearly illustrates the need for a huge storage space, large transmission bandwidth and long transmission time for a 1 minute video. Hence in order to reduce the

[2] Image source: Internet: http://www.engr.usask.ca/classes/CME/462/

required amount of storage and transmission bandwidth, it is necessary to compress the image or video.

1.3.2 Principle of data compression

The main principle behind the image/data compression technique is to reduce the redundancy. In image compression methodology, generally spectral and spatial redundancy should be reduced as much as possible while for video compression, the temporal redundancy should be reduced. In this work, the still images and the video sequences (as a group of still images) are considered for the analysis. The compression is achieved by reducing the spatial redundancy of the image/frame data.

1.3.3 Classification of data compression

The data compression techniques are mainly classified into two groups as follows:

I. Lossless compression technique

II. Lossy compression technique

I. ***Lossless compression technique***

In the lossless data compression techniques, the original data can be exactly reconstructed as the original data. This type of compression techniques are generally used where the reconstruction quality is of the utmost importance, such as, executable programs, text documents, and source codes. Some example of lossless compression techniques are:

a. Zip file format, and

b. Tiff image format

II. ***Lossy compression technique***

The lossy compression techniques achieve data compression by losing some information while maintaining the reconstruction quality. Hence, the data cannot be reconstructed exactly as the original one. This is used for applications where low storage space and fast data transmission speed are needed while maintaining the acceptable reconstructed data quality. The examples of such applications are still image compression, video conferencing, internet telephony and so on. Some example of lossy compression techniques are as follows.

a. JPEG

b. JPEG 2000

1.4 Literature review

The Joint Photographic Expert Group (JPEG) standard was developed in 1992, based on the Discrete Cosine Transform (DCT). It has been one of the most popular and widely used compression methods [3, 4]. Although hardware implementation for the JPEG using the DCT is simple, the noticeable "blocking artifacts" across the block boundaries cannot be neglected for higher compression ratio. In addition, the quality of the reconstructed images is degraded by the "false contouring" effect for specific images having gradually shaded areas [5]. The false contouring occurs when smoothly graded area of an image is distorted by an aberration due to heavy quantization of the transform coefficients. The effect looks like a contour map. The Discrete Wavelet Transform (DWT) based coding, on the other hand, has been emerged as another efficient tool for image compression [6-8], mainly due to its ability to display image at different resolutions and to achieve higher compression ratio. The Embedded Zero Tree Wavelet coefficients (EZW) coding has been introduced by Shapiro in [9]. In order to obtain higher resolution more scales are required in EZW, which in turn increases the complexity of the algorithm. Hence, in [10] another coding technique: Set Partitioning in Hierarchical coding Techniques (SPIHT) has been developed, which outperforms the EZW in terms of compression efficiency and the speed. However, the SPIHT coding is considered to be less efficient than the JPEG 2000 standard [11, 12]. Therefore, Set partitioning Embedded Block Coder (SPECK) is developed in [13]. Later on, modified version of SPECK for the higher complexity has been developed in [14].

Discrete Walsh Hadamard Transform (DWHT) is another option for the image and video compression applications which requires less computation as compared to DCT and DWT algorithm. In [15], authors used DWHT algorithm to compress video. However, the performance of the DWHT is suitable only for the lower compression levels. For the higher compression ratio, the performance of DWHT reduces drastically. In order to benefit from the respective strengths of individual popular coding schemes, a new scheme, known as hybrid-algorithm, has been developed where two transforms techniques are implemented together. There have been few

efforts devoted to such hybrid implementation. In [16], the authors have presented a hybrid transformation scheme for video coding, which minimizes prediction error. The DWT is used for intra-coding and the DCT for intercoding. Usama presents a scalable hybrid scheme for image coding that combines both the Wavelet and the Fourier transforms [17]. Simulation results demonstrate that, with small addition in the computational complexity of the coding process, the PSNR performance of the algorithm is higher than that of the SPIHT (set partitioning in hierarchical trees) test coder and some other image coding techniques. An extended version of the object-based coding algorithm is presented in [18]. Yu and Mitra in [19] have introduced another form of hybrid transformation coding technique. The EZW coding is applied on the first level wavelet coefficients and the arithmetic coding has been implemented to generate the symbol stream. In [20], Singh et al. have applied similar hybrid algorithm to medical images that uses 5-level DWT decomposition. Because of higher level (5 levels DWT), the scheme requires large computational resources and is not suitable for use in modern coding standards.

The concept of combining multiple transforms is getting popular in recent years as researchers have put effort in developing schemes with various different discrete transforms. For example, the authors in [21] present a scalable algorithm for video coding where the DWT is performed on the DCT coefficients. The work in [22] presents a hybrid architecture where three popular transforms (i.e., Discrete Fourier transform (DFT), Discrete Cosine Transform (DCT), and the Haar Transform) have been implemented on a single chip. The work in [23] presents similar but a more efficient hybrid scheme where the three same transforms have been implemented using the structural similarity and resource sharing. Moreover, the Fourier-Wavelet Transform can be used to improve the de-noising performance for images [24]; a Cosine-Wavelet hybrid structure can be used to enhance the security in digital watermarking [25], etc. There have been some reports on multiple IDCT implementations to support multiple standards [26-28], that result in improved performance.

1.5 Motivation and objectives of the thesis

Data compression is one of the major areas of the research in image and video processing applications. With the development of computer and internet technology, more multimedia-based information is being transmitted over the internet and wireless networks. The raw data to be

transmitted consumes large bandwidth and requires huge storage space; as a result, it is desirable to represent the information in the data with considerably fewer bits by the mean of data compression techniques. At a same time, the data compression technique must be able to reconstruct the data very close to original data. This can be achieved via an effective and efficient compression and decompression algorithms.

The DCT and DWT are the most commonly used algorithms. The DCT has high energy compaction property and requires less computational resources. The energy compaction property of an algorithm refers to the ability to concentrate most important information signal into as much as few low frequency component. On the other hand, DWT is a multi-resolution transform and variable compression can be easily achieved. The main disadvantages of DCT are introduction of false contouring effects and blocking artifacts at higher compression, and, that of DWT is requirement of large computational resources. So, the idea of exploring the advantages of both algorithms motivated us to investigate combination of DWT and DCT algorithms. Such combination of two algorithms is referred as '*hybrid*' algorithm.

In case of stand-alone DWT, to achieve higher compression, higher level of DWT decomposition stages need to be considered. This will increase the computational complexity, and, degrades the reconstruction quality. On the other hand, in case of stand-alone DCT, the data block size is smaller compared to DWT, which means, higher number of blocks need to be processed for same size of image. The compression in DCT can only be achieved by quantization and scaling. Higher scaling factor will be needed to achieve higher compression. This degrades the reconstruction quality of each block. Blocking artifact may appear due to the higher numbers of blocks used. The detail explanation of blocking artifact effect is presented in Section 2.2.1.

In this research work, we present a hybrid algorithm: 2-level 2-D DWT followed by 8×8 2-D DCT. The 2-D DWT will be applied on 32×32 data block of an image. The main advantage of applying two stage of DWT is to achieve high compression while maintain reconstruction quality. Furthermore, motivation behind applying DCT to the DWT coefficients (after two level of DWT), is to represent the most important information in few low frequency components. Further compression can be achieved by using quantization and scaling on DCT coefficients. Since, the large data block size is considered compared to stand-alone DCT; there will be less probability of occurrence of the blocking artifact.

The main objective of this research work is to investigate the performance of proposed hybrid algorithm for wide range of image and video applications at various compression levels. The detail of proposed hybrid algorithm is presented in Chapter 3.

1.6 Scope of the research work

The proposed research work has following scopes.

I. The proposed algorithm can be used for real time applications such as video conferencing, telemedicine, where, fast transmission is desired.

II. The proposed algorithm can also be a good option for the image processor of the wireless capsule endoscopic system.

1.7 Organization of thesis

In Chapter 1, the basics of image and video have been introduced. The chapter briefly described the image types and stated the purpose of image and video compression in this digital era. In addition, an introduction to principle of data compression and its technique is presented. Furthermore, the motivations towards this works and the objective of this thesis work have been presented. Finally the scope of the thesis is stated in this chapter.

Chapter 2 presents a brief introduction of commonly used transform techniques for the data compression. The Discrete Cosine Transform (DCT), the Discrete Wavelets Transform (DWT), and the Walsh Hadamard Transform (WHT) have been described. The advantage and disadvantage of all these algorithms are further presented in this chapter.

In order to compensate the drawback of each other and utilize the advantages of each algorithm, a hybrid DWT-DCT algorithm has been introduced in this thesis work. Chapter 3 deals with the detailed analysis of the proposed hybrid algorithm under consideration. Furthermore, the advantages and the applications of proposed hybrid algorithm are also illustrated in this chapter.

Once the algorithm is prepared, it is necessary to analyze the result using various evaluation parameters. In order to analyze the performance of the proposed algorithm, both subjective and objective evaluation parameters have been considered in Chapter 4.

All the analysis has been performed using MATLAB tool. The simulation results and the comparisons are presented in Chapter 5. In addition, the proposed hybrid algorithm is compared with some already developed schemes.

Finally, Chapter 6 concludes the works with brief outline of the future work.

CHAPTER 2
TRANSFORM TECHNIQUES FOR IMAGE/VIDEO COMPRESSION

2.1 Introduction

Image/Video is digitally represented in a set of pixel. Generally the neighbouring pixels are correlated to each other and are redundant in nature. The redundancy unnecessarily occupies storage space which in turn increases the transmission cost and the bandwidth of the system. Hence, it is necessary to reduce the redundancy of an image/video. The reduction in redundancy can be achieved by means of data compression techniques. The main idea behind the compression technique is to use orthonormal transformation making the pixel value smaller than the original. The transformation of the data also makes the coefficients of the transformed matrix uncorrelated to each other. There are various methods of transformations being used for data compression as follows:

i. Karhunen-Loeve Transform (KLT)

ii. Discrete Fourier Transform (DFT)

iii. Discrete Sine Transform (DST)

iv. Walsh Hadamard Transform (WHT)

v. Discrete Cosine Transform (DCT)

vi. Discrete Wavelet Transform (DWT)

Karhunen-Loeve Transform: Among the above transformation techniques, KLT is the optimal transformation technique which always results exactly uncorrelated transformed coefficients [30]. Moreover, KLT has the minimum mean square error as compared to other transformation techniques [31]. It also has high energy compaction property i.e. it keeps as much energy as possible in few coefficients. However, one of the drawback of KLT is it is non separable transformation thus; it requires large computational resources as compared to other transformation techniques.

Discrete Fourier Transform: DFT is linear, separable and symmetric. It also exhibits good decorrelation and energy compaction characteristics but less compared to DCT.

Example 2.1: *Energy compaction comparison of DFT with DCT*

Let us take a highly correlated input sequence $A = [8,16,24,32,40,48,56,64]$ [32] as shown in Figure 2.1. When DFT is applied to this input, it can be seen that the transformed output is not decorrelated. It is also clear that the output after taking inverse DFT is highly deviated from the original data. On the other hand, when DCT is applied to the given input, it can be seen that all the energy is concentrated in the first element and rest are of very less value i.e. data are significantly decorrelated. The output after taking inverse of DCT is identical to the input data even though neglecting some of the components during quantization. It shows the advantage of using DCT over DFT.

Furthermore, DFT is complex transformation and requires computation of both magnitude and phase information. In addition, DFT gives rise to boundary discontinuities (Gibb's phenomena) due to implicit periodicity [33].

Discrete Sine Transform: The DST is another option for data compression but it produces the reduced quality reconstruction as compared to DCT. This is due to the fact that the DST does not yields DC coefficient and have only the AC coefficient i.e. there is less degree of energy compaction [33].

Walsh Hadamard Transform: The WHT is another method for data compression. It is fast since it requires only the addition and subtraction. However, it has very low energy compaction characteristics as compared to DCT.

Discrete Cosine Transform: The performance of DCT is very close to the Karhunen-Loeve Transform (KLT) and requires less computational complexity [34]. In addition, DCT has property of higher energy compaction [35] compared to DFT, DST, WHT and DWT. Hence, DCT is generally used for image and video compression. However, for the higher compression, it introduces blocking artifacts and the contour effects in reconstructed image. Besides that, it is not the multi-resolution transformation technique.

Discrete Wavelet Transform: DWT is multi-resolution transform technique, generally used for image and video compression to achieve higher compression ratio.

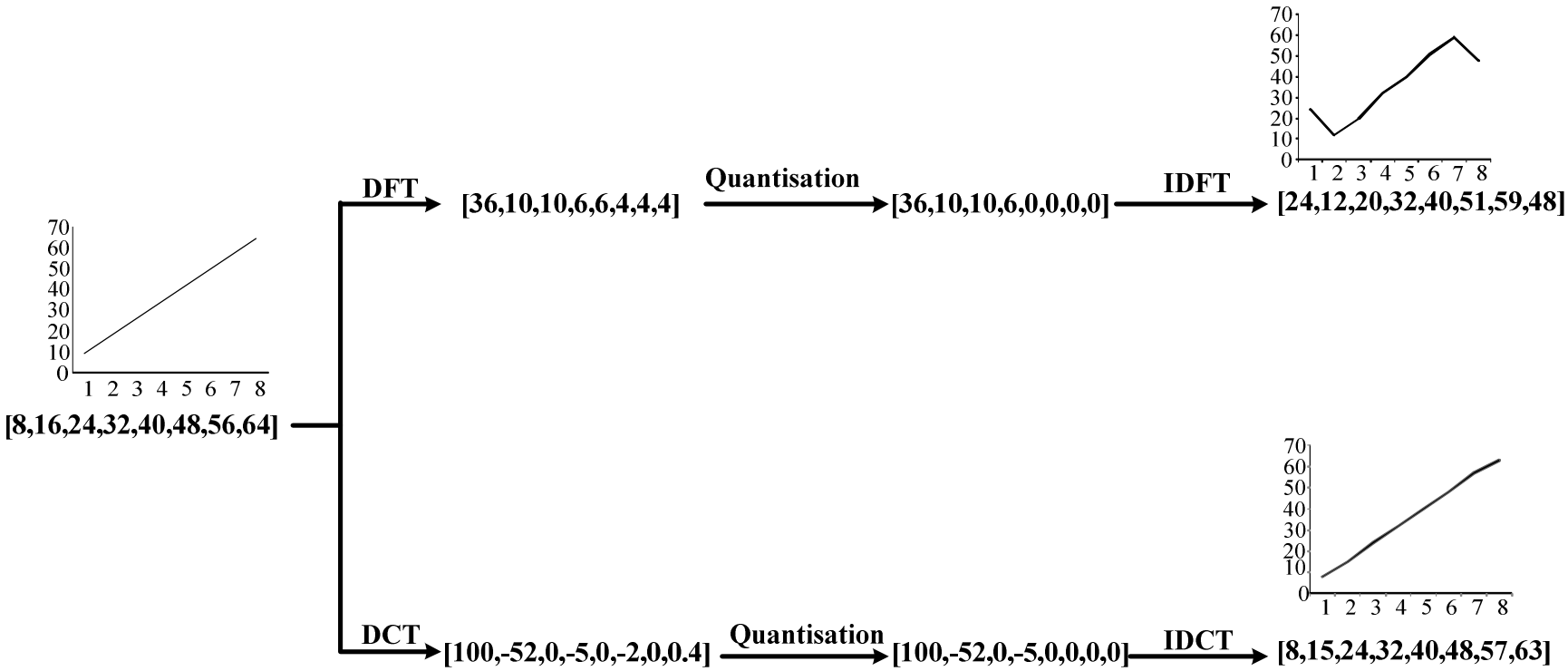

Figure 2.1. DFT and DCT energy compaction characteristics

Multiple transformation methods can be used in order to compensate the drawbacks of each other. The proposed hybrid algorithm, which is explained in next chapter, uses combination of DCT and DWT techniques for image and video compression. Therefore, in this chapter, the detailed description of DCT and DWT are presented.

2.2 Discrete Cosine Transform (DCT)

A DCT represents the input data points in the form of a sum of cosine functions that are oscillating at different frequencies and magnitudes. There are mainly two types of DCT: one dimensional (1-D) DCT and two dimensional (2-D) DCT. Since an image is represented as a two dimensional matrix, for this research work, 2-D DCT is considered. The 2-D DCT for an $N \times N$ input sequence can be defined as follows [35]:

$$D_{DCT}(i,j) = \frac{1}{\sqrt{2N}} B(i)B(j) \sum_{x=0}^{N-1} \sum_{y=0}^{N-1} M(x,y) \cos\left[\frac{2x+1}{2N} i\pi\right] \cos\left[\frac{2y+1}{2N} j\pi\right] \tag{2.1}$$

where,

$$B(u) = \begin{cases} \frac{1}{\sqrt{2}} & if \quad u = 0 \\ 1 & if \quad u > 0 \end{cases}.$$

$M(x,y)$ is the input data of size $x \times y$. In the DCT compression, almost all of the information is concentrated in a small number of the low frequency coefficients. These low frequency coefficients are also known as DC components and the rest of the components are AC components. The DCT coefficients are then quantized using a 8×8 quantization table, Q [36], as described in the Joint Photographic Expert Group (JPEG) standard. The quantization is achieved by dividing each element of the transformed data by corresponding element in the quantization matrix Q and rounding to the nearest integer value as shown in Eq. (2.2).

$$D_{quant}(i,j) = round\left(\frac{D_{DCT}(i,j)}{Q(i,j)}\right) \tag{2.2}$$

Further compression can be achieved by applying appropriate scaling factor. In order to reconstruct the output data, the rescaling and the de-quantization should be performed as given in Eq. (2.3).

$$D_{dequant}(i,j) = Q(i,j) \times D_{quant}(i,j) \tag{2.3}$$

The de-quantized matrix is then transformed back using the 2-D inverse-DCT [35]. The equation for the 2-D inverse DCT transform is given in the Eq. (2.4).

$$D_{IDCT}(i,j) = \frac{1}{\sqrt{2N}} \sum_{x=0}^{N-1} \sum_{y=0}^{N-1} B(i)B(j)D_{dequant}(i,j) \cos\left[\frac{2x+1}{2N} i\pi\right] \cos\left[\frac{2y+1}{2N} j\pi\right] \tag{2.4}$$

where,

$$B(u) = \begin{cases} \frac{1}{\sqrt{2}} & if \quad u = 0 \\ 1 & if \quad u > 0 \end{cases}$$

Example 2.2: A DCT compression and reconstruction procedure

Let us take a random input data of 8×8 matrix representing a portion of image as shown in Figure 2.2. The transform coefficients as shown in Figure 2.3 can be obtained by applying 2-D DCT to a given input matrix. The element at upper left corner shown in bold is the DC component (low frequency) having highest value. Rest of the other elements are the ac components (high frequency). Human eye is more sensitive to the DC component and less sensitive to AC component. Hence, the AC component can be neglected in order to achieve higher compression- by passing the transformed data through the quantizer.

48	47	40	50	60	38	50	90
100	95	80	98	110	106	30	60
70	63	83	69	112	107	74	125
85	97	78	58	72	76	91	66
25	36	33	50	66	61	40	38
135	108	85	106	116	61	75	92
140	134	134	98	107	158	161	109
212	104	60	44	61	136	110	66

Figure 2.2. A random value input data

673.625	17.8418	28.6303	61.8853	10.875	-17.019	15.8772	1.2883
-115.28	-36.517	-54.836	-60.931	35.8779	-45.415	2.2054	-4.3304
56.0184	21.064	48.005	39.0992	-0.5687	18.003	18.9836	-10.352
-55.806	0.1755	-28.28	-46.339	27.3306	-4.0105	-31.386	3.6849
-126.63	-5.3299	33.7428	16.8063	-12.375	17.3996	-10.324	-1.9576
64.1123	-35.849	25.3665	-32.869	-35.859	10.4856	-13.577	19.3289
-22.527	-11.076	29.9836	-10.094	46.6431	-5.3347	-0.255	13.4784
-35.738	-66.689	-18.381	-10.739	-13.511	-5.7672	16.7621	1.3709

Figure 2.3. Transformed coefficients after DCT of the random value input data

The JPEG quantization table is shown in Figure 2.4. The corresponding value after quantization is as shown in Figure 2.5. We can see that more than 70 percent of the coefficients are quantized to zero. Further compression can be achieved by the use of scaling factor (*SF*) to the quantized coefficients. The reconstructed data after inverse transformation is illustrated in Figure 2.6. There is a small deviation between the input data and output data due to the quantization. The entire DCT procedure is shown in Figure 2.7.

16	11	10	16	24	40	51	61
12	12	14	19	26	58	60	55
14	13	16	24	40	57	69	56
14	17	22	29	51	87	80	62
18	22	37	56	68	109	103	77
24	35	55	64	81	104	113	92
49	64	78	87	103	121	120	101
72	92	95	98	112	100	103	99

Figure 2.4. JPEG Quantization table

42	2	3	4	0	0	0	0
-10	-3	-4	-3	1	-1	0	0
4	2	3	2	0	0	0	0
-4	0	-1	-2	1	0	0	0
-7	0	1	0	0	0	0	0
3	-1	0	-1	0	0	0	0
0	0	0	0	0	0	0	0
0	-1	0	0	0	0	0	0

Figure 2.5. Quantized coefficients

45.2748	54.7023	46.5615	56.6765	69.6439	36.7503	35.6914	98.143
102.687	94.7849	62.8007	65.4573	102.692	89.2906	46.2655	38.8075
62.2915	85.1708	80.9425	80.7011	114.635	130.659	113.858	102.692
71.0696	89.3584	88.1848	70.1445	61.7288	61.3081	61.7905	64.8018
44.765	25.8218	26.6467	45.5859	56.1577	59.1172	60.605	58.5792
132.787	101.999	103.815	115.072	94.9821	77.3537	73.8953	64.5329
149.547	119.257	117.593	120.235	113.372	139.334	158.981	135.509
208.546	125.353	57.7344	34.7159	63.807	133.437	128.937	42.3605

Figure 2.6. Reconstructed output data

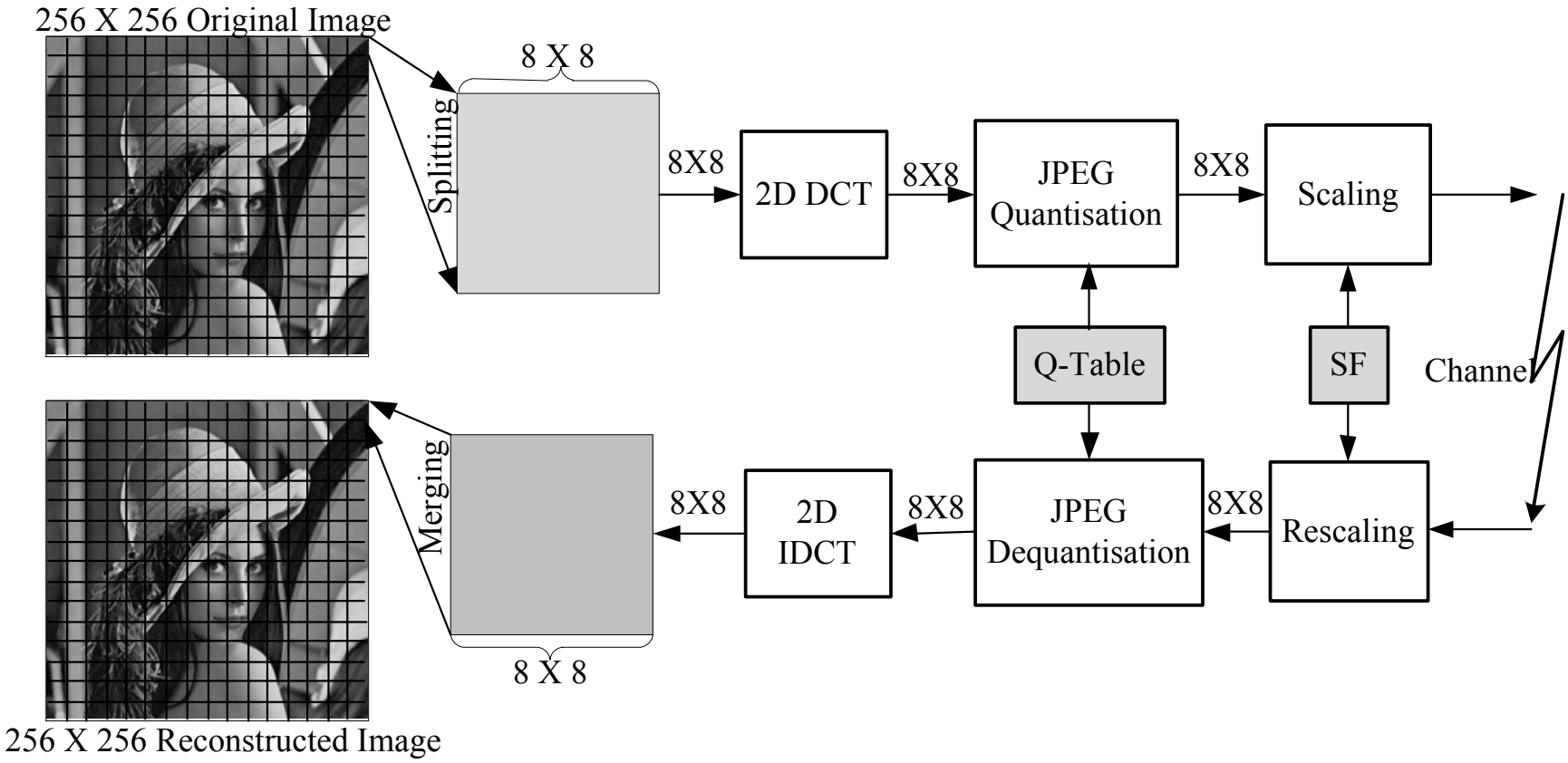

Figure 2.7. Block diagram of the JPEG-based DCT

2.2.1 Limitations of DCT

Figure 2.8 and 2.9 shows the original image and reconstructed images at two different compression level using 2- D DCT. For the lower compression ratio, the distortion is unnoticed by human visual perception, which can be seen in Figure 2.8-(b). In order to achieve higher compression it is required to apply quantization followed by scaling to the transformed coefficient. For such higher compression ratio DCT has following two limitations.

1. ***Blocking artifacts***: Blocking artifacts is a distortion that appears due to heavy compression and appears as abnormally large pixel blocks. For the higher compression ratio, the noticeable "blocking artifacts" across the block boundaries cannot be neglected. The example of appearance of blocking artefact due to high compression is shown in Figure 2.8-(c).
2. ***False contouring:*** The false contouring occurs when smoothly graded area of an image is distorted by an aberration that looks like a contour map for specific images having gradually shaded areas [5]. The main cause of the false contouring effect is the heavy quantization of the transform coefficients. An example of false contouring can be observed in Figure 2.9-(c).

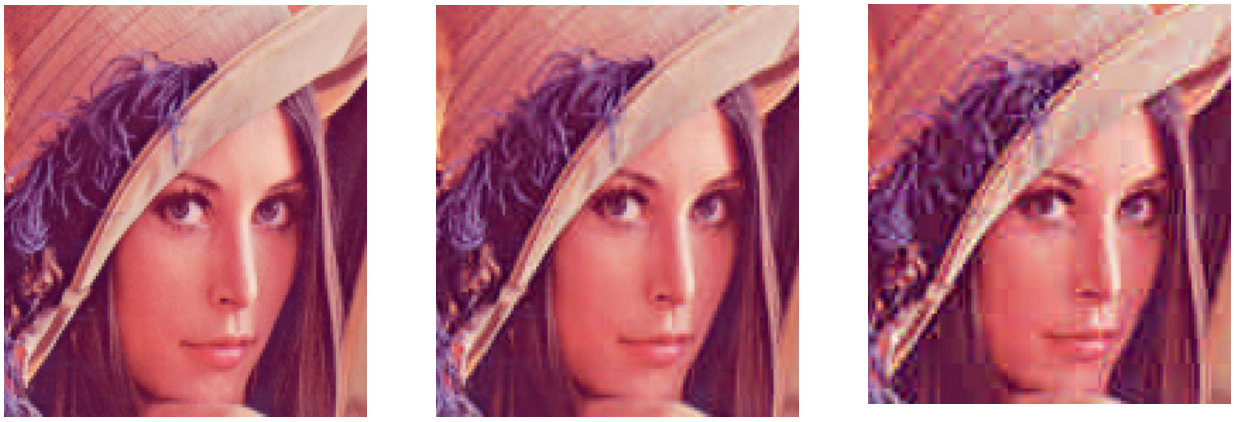

(a) (b) (c)

Figure 2.8. Illustration of compression using DCT: (a) Original Image[1], *CR* at (b) 88%, (c) 96%

1 Image source: Internet: http://sipi.usc.edu/database/index.html.

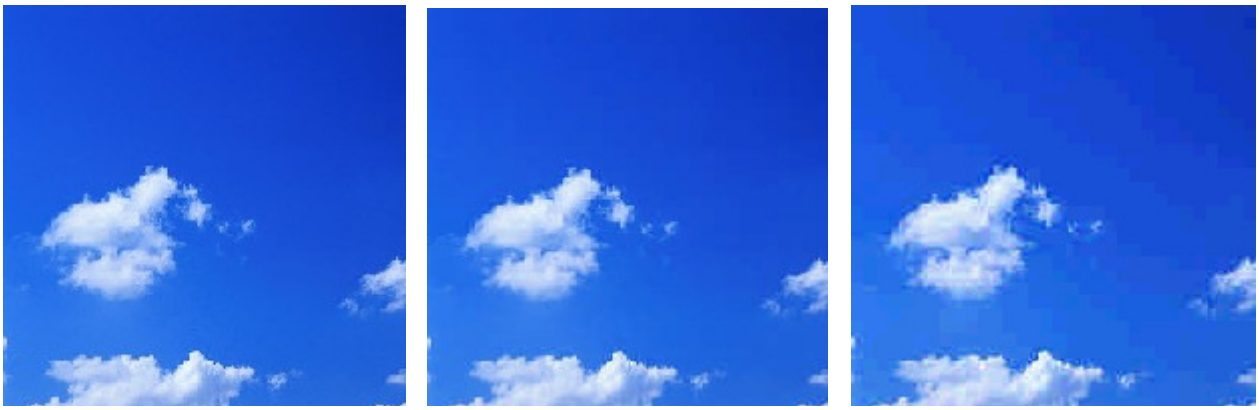

(a) (b) (c)

Figure 2.9. Illustration of compression using DCT: (a) Original Image[2], *CR* at (b) 87 %, (c) 97%

2.3 Discrete Wavelet Transform (DWT)

The DWT represents an image as a sum of wavelet functions, known as *wavelets*, with different location and scale [8]. It represents the data into a set of high pass (detail) and low pass (approximate) coefficients. The input data is passed through set of low pass and high pass filters. The Daubechies filter coefficients [37] are used for in this work. Filter kernel used for this research work is $\begin{bmatrix} 1 & 1 \\ 1 & -1 \end{bmatrix}$. The output of high pass and low pass filters are down sampled by 2. The output from low pass filter is an approximate coefficient and the output from the high pass filter is a detail coefficient. This procedure is one dimensional (1-D) DWT and Figure 2.10 shows the schematics of this method.

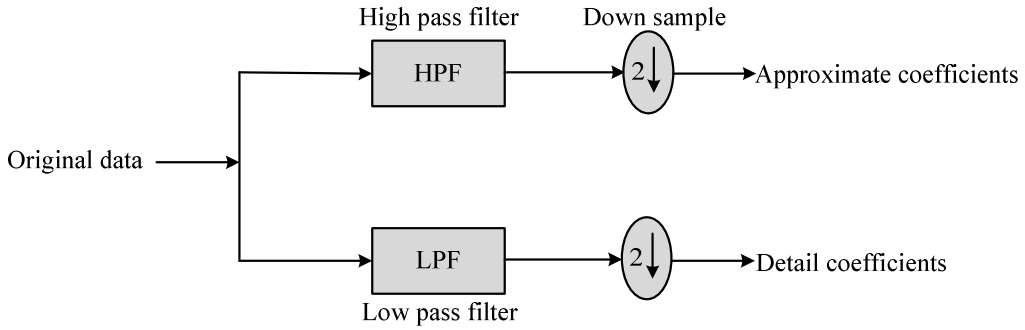

Figure 2.10. Block diagram of 1-D forward DWT

2 Image source: campbelltown.nsw.gov.au

In case of 2-D DWT, the input data is passed through set of both low pass and high pass filter in two directions, both rows and columns. The outputs are then down sampled by 2 in each direction as in case of 1-D DWT. The complete process is illustrated in Figure 2.11. As shown in Figure 2.11, output is obtained in set of four coefficients LL, HL, LH and HH. The first alphabet represents the transform in row where as the second alphabet represents transform in column. The alphabet L means low pass signal and H means high pass signal. LH signal is a low pass signal in row and a high pass in column. Hence, LH signal contain horizontal elements. Similarly, HL and HH contains vertical and diagonal elements, respectively.

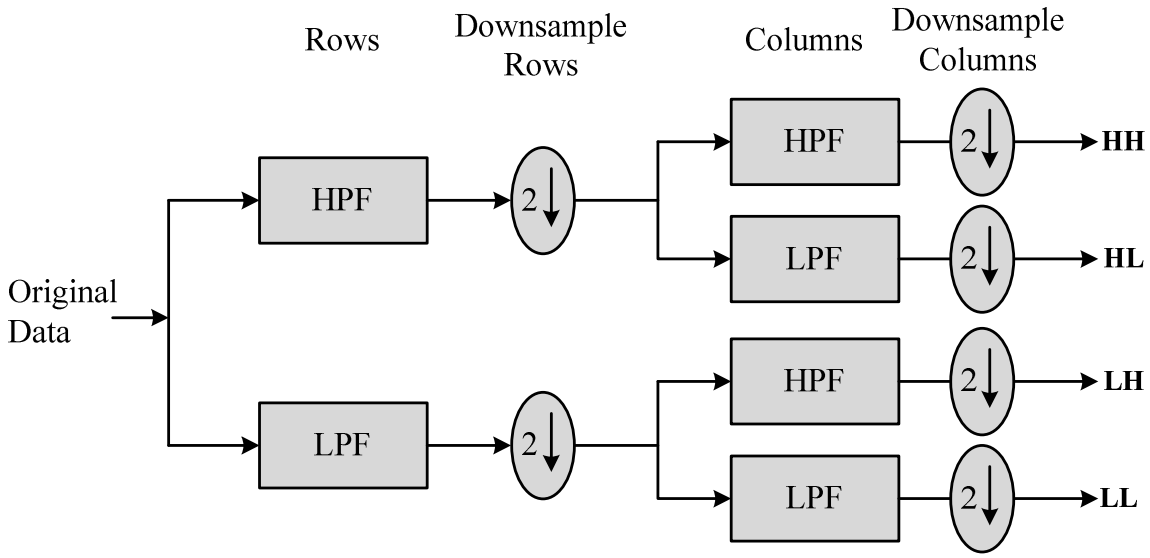

Figure 2.11. Block diagram of 2-D forward DWT

In DWT reconstruction, input data can be achieved in multiple resolutions [38] by decomposing the LL coefficient further for different levels as shown in Figure 2.12. In order to reconstruct the output data, the compressed data is up-sampled by a factor of 2. The signal is further passed through the same set of high pass and low pass filter in both rows and columns. The entire reconstruction procedure is shown in Figure 2.13.

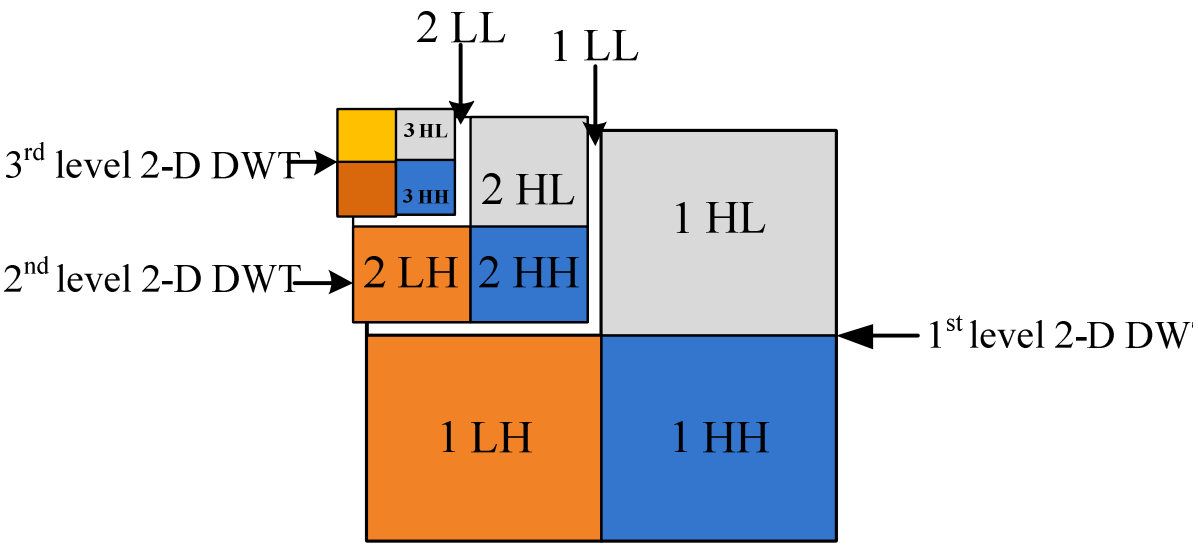

Figure 2.12. Illustration of forward DWT

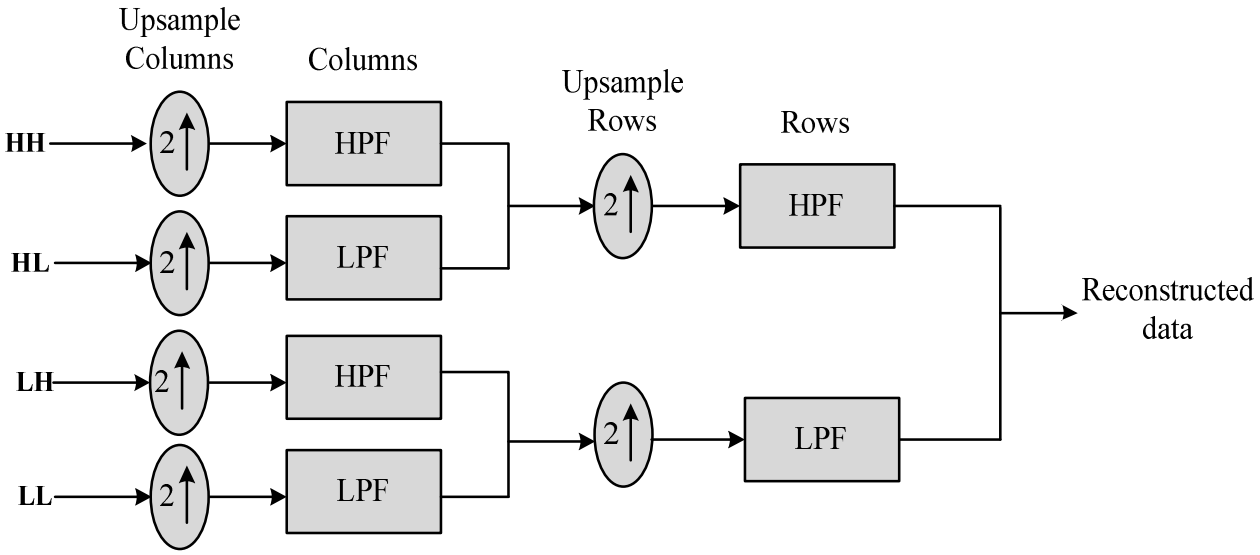

Figure 2.13. Block diagram of 2 dimensional inverse DWT

In this research work, an image is first divided into blocks of 32×32. Each block is then passed through the two filters: high pass filter and low pass filter. The first level decomposition is performed to decompose the input data into an approximation and the detail coefficients. After obtaining the transformed matrix, the detail and approximate coefficients are separated as LL, HL, LH, and HH coefficients. All the coefficients are discarded, except the LL coefficients. The LL coefficients are further transformed into the second level as shown in Figure 2.14. The process continues for one more level. The coefficients are then divided by a constant scaling factor (SF) to achieve the desired compression ratio. Finally, for data reconstruction, the data is rescaled and padded with zeros, and passed through the wavelet filters. The entire process of 2-D DWT compression and reconstruction is shown in Figure 2.15.

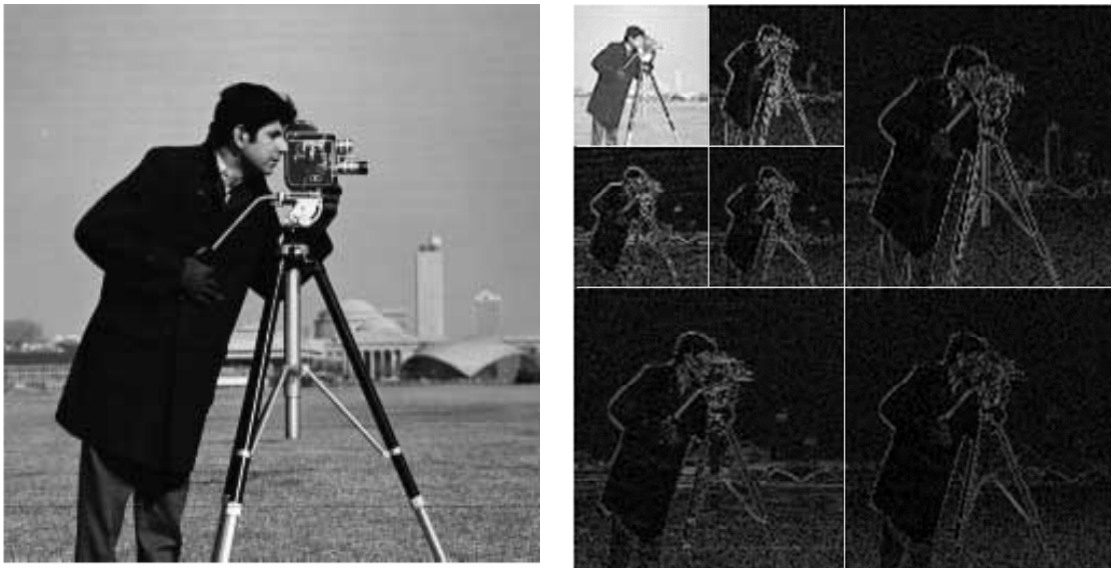

Figure 2.14. Illustration of 2 dimensional DWT for an image 'Cameraman'[3]

[3] Image source: Internet: http://sipi.usc.edu/database/index.html.

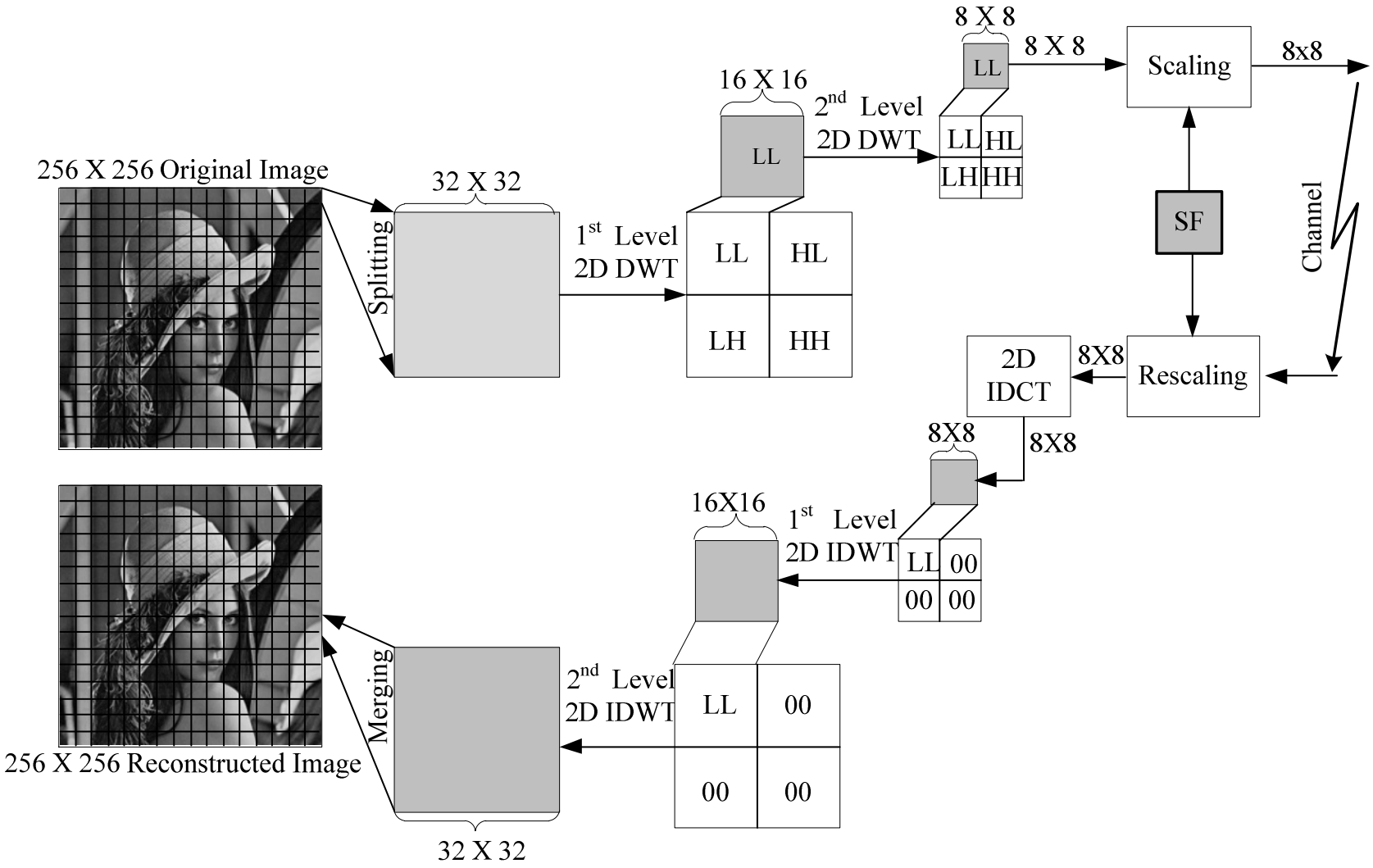

Figure 2.15. Block diagram of the DWT decomposition

Example 2.3: DWT compression and reconstruction procedure

For this example the input data is consider as 8×8 matrix as presented in Example 2.2. After applying 2 D DWT to the given input, the transform coefficients are obtained in group of LL, LH, HL and HH coefficient as described above. These coefficients are shown in Figure 2.16. It is clear that the all the low frequency components are concentrated in right top most corner. These are the LL coefficients. The LH, HL, and HH coefficients are of very low in values and hence can be neglected to achieve higher compression. To achieve higher compression ratio, any of the coefficients of LH, HL, and HH coefficients can be neglected. For example, to achieve 50% compression ratio, the HL and HH coefficients are padded with zeros as shown in Figure 2.17. The inverse DWT of this data is shown in Figure 2.18. Due to the compression, the reconstructed data are deviated from the input value with very small error.

LL coefficient				**LH coefficient**			
145	134	157	115	-50	-44	-59	25
157.5	144	183.5	178	-24.5	8	35.5	21
152	137	152	122.5	-91	-54	-25	-44.5
295	168	231	223	-21	64	34	47
3	-14	13	-35	-2	4	9	-5
-2.5	17	0.5	-13	9.5	-3	4.5	-38
8	-19	30	-7.5	-19	2	-25	9.5
57	26	-63	48	-51	10	12	4
HL coefficient				**HH coefficient**			

Figure 2.16. Transformed coefficient after 2-D DWT

LL coefficient				LH coefficient			
145	134	157	115	-50	-44	-59	25
157.5	144	183.5	178	-24.5	8	35.5	21
152	137	152	122.5	-91	-54	-25	-44.5
295	168	231	223	-21	64	34	47
0	0	0	0	0	0	0	0
0	0	0	0	0	0	0	0
0	0	0	0	0	0	0	0
0	0	0	0	0	0	0	0
HL coefficient				**HH coefficient**			

Figure 2.17. Zero padding

47.5	47.5	45	45	49	49	70	70
97.5	97.5	89	89	108	108	45	45
66.5	66.5	76	76	109.5	109.5	99.5	99.5
91	91	68	68	74	74	78.5	78.5
30.5	30.5	41.5	41.5	63.5	63.5	39	39
121.5	121.5	95.5	95.5	88.5	88.5	83.5	83.5
137	137	116	116	132.5	132.5	135	135
158	158	52	52	98.5	98.5	88	88

Figure 2.18. Reconstructed output of input data (Example 2.2) obtained after 2-D IDWT

2.4 Walsh Hadamard Transform (WHT)

The forward Walsh Hadamard Transform (WHT) is given by:

$$y_n = \frac{1}{N}\sum_{i=0}^{N-1} x_i H(n,i)$$

Where, N must be power of 2. i.e. $N = 2^n$. $H(n,i)$ is the walsh function and can be defined as,

$$(H_m)_{k,n} = \frac{1}{2^{\frac{m}{2}}}(-1)^{\sum_j k_j n_j}$$

For 1×1, 2×2 matrix, and so on, the hadamard coefficient is defined as below respectively,

$$H_0 = +1$$

$$H_1 = \frac{1}{\sqrt{2}}\begin{bmatrix} 1 & 1 \\ 1 & -1 \end{bmatrix}$$

The inverse Walsh Hadamard Transform is defined as below:

$$x_i = \sum_{i=0}^{N-1} y_n H(n,i)$$

Example 2.4: WHT compression efficiency

A standard image 'Yatch' is compressed using WHT at different compression level is shown in Figure 2.19. It is clearly observed that for the lower compression ratio, the WHT performs well. However for higher compression ratio, the reconstruction quality of the WHT is drastically degraded. This property of the WHT is visually illustrated in Figure 2.19.

2.4.1 Advantage of WHT

Since the coefficient of Walsh Haddamard Transform consists of 0's or 1's, it is easier to implement as compared to DCT and other transform techniques. Being a binary in nature, it just

needs additions and subtraction .i.e. no multiplication is required [39], [40] which reduces the computational complexity.

(a) Original image (b) *PSNR* = 37.73dB (c) *PSNR* = 28.34dB

Figure 2.19. WHT reconstruction quality (a) original image [1](b) *CR*=65.75%, (b) *CR*=82%

2.4.2 Limitation of WHT

Although, the computational complexity of WHT is simpler than other transform techniques, it is not suitable for the application which requires higher compression ratio. For the higher compression ratio, the reconstruction quality drastically decreases as seen in the Figure 2.19.

2.5 Summary

In this chapter, various methods of transformation methodology for data compression such as KLT, DST, DCT, DWT, WHT has been presented. KLT is the optimal transformation having highest energy compaction property. Despite the fact, it requires large computational resources. DCT requires less computational resources and can achieve the energy compaction property as KLT. However, for the higher compression ratio it introduces the blocking artifacts and the false contouring effects while image reconstruction. WHT requires lesser computational resources

[1]Image source: http://r0k.us/graphics/kodak/kodim09.html

than the DCT but has less energy compaction property and is not suitable for the higher compression ratio. Both DCT and WHT technique does not show the multi-resolution compression property. DWT is the only techniques which has capacity of multi resolution compression. However, it requires higher computational complexity as compared to other techniques. Hence, in order to benefit from each other, hybrid DWT-DCT algorithm has been developed for the image and video compression in this thesis work and is explained in the following chapter.

CHAPTER 3
PROPOSED HYBRID DWT-DCT ALGORITHM

3.1 Introduction

For the lower compression ratio, the DCT algorithm shows higher energy compaction characteristics and requires less computational complexity as compared to other compression methods: DFT, DST, WHT, and DWT. However, it introduces the blocking artifacts and the false contouring effect at the higher compression ratio. Furthermore it is not a multi-resolution technique. On the other hand, DWT is multi-resolution compression method i.e. an image can be obtained in different resolutions by discarding the detail coefficients and taking only the approximate coefficient. But, the energy compaction characteristic of DWT is less as compared to DCT and requires more computational processor. Hence, multiple transform can be implemented in order to compensate the drawback of each other. In this research work, a hybrid DWT-DCT algorithm has been proposed.

In preliminary work [41], the medical image of any size that can be divisible by 16 is considered for the analysis. The image is divided into 16×16 blocks and the entire hybrid DWT-DCT algorithm was implemented. The analysis shows that proposed hybrid DWT-DCT algorithm has better performance as compared to stand alone DWT and DCT in terms of Peak Signal to Noise Ratio (*PSNR*) and Compression Ratio (*CR*).

The only limitation of this preliminary work is use of the lower block size and the analysis was performed on the medical images. Hence, in order to improve the limitation, the proposed hybrid DWT DCT algorithm is implemented for the increased block size of 32×32. In this chapter, the improvised proposed Hybrid DWT-DCT algorithm has only been explained since the entire algorithm for both works is similar.

3.2 Hybrid DWT-DCT algorithm

3.2.1 The process of data compression

Given consideration of the type of application, the original image/frame of size 256×256 (or any resolution, provided divisible by 32) is first divided into blocks of size 32×32. Each 32×32 block is then decomposed using the 2-D DWT. The high-frequency coefficients HL, LH, and HH are discarded. At this level, seventy five percent of data are compressed. The low-frequency coefficients (LL) are passed to the next stage. The passed LL components are further decomposed using 2-D DWT. The compression level can be adjusted by applying various DWT sub sampling methods. The concepts of DWT sub sampling is pictorially explained in Figure 3.1. Figure 3.1-(a) shows the fully sampled DWT sub sampling, (b) shows the quarterly sampled DWT sub sampling and (c) shows the half sampled DWT sub sampling.

Fully sampled DWT sub sampling: In this method of DWT sub sampling, all the LL, HL, LH, and HH coefficients are taken into consideration.

Quarterly sampled DWT sub sampling: In this method of DWT sub sampling, all the HH coefficients are discarded.

Half sampled DWT sampling: Similarly, by the half sampled DWT sub sampling, means taking odd and even coefficients from either HL, or HL set and discarding the HH coefficients.

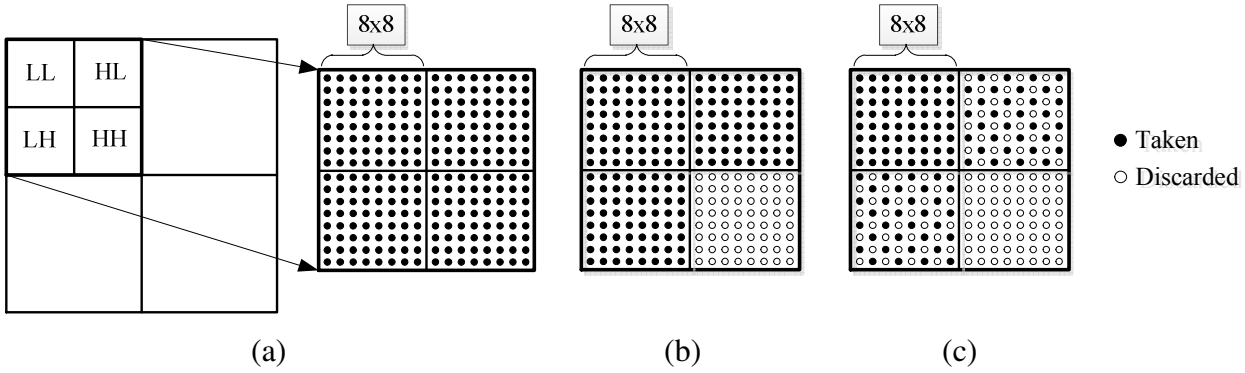

Figure 3.1. Sub-sampling of the DWT coefficients: (a) fully sampled; (b) quarterly sampled; (c) half sampled

After the DWT sub sampling, the 8-point DCT is applied to these DWT coefficients. To achieve further compression, a JPEG-like quantization is performed. In this stage, most of the higher frequency components are rounded to zero. The quantized coefficients are further scaled using scalar quantity known as scaling factor (*SF*). The entire hybrid DWT-DCT compression process is illustrated in Figure 3.2.

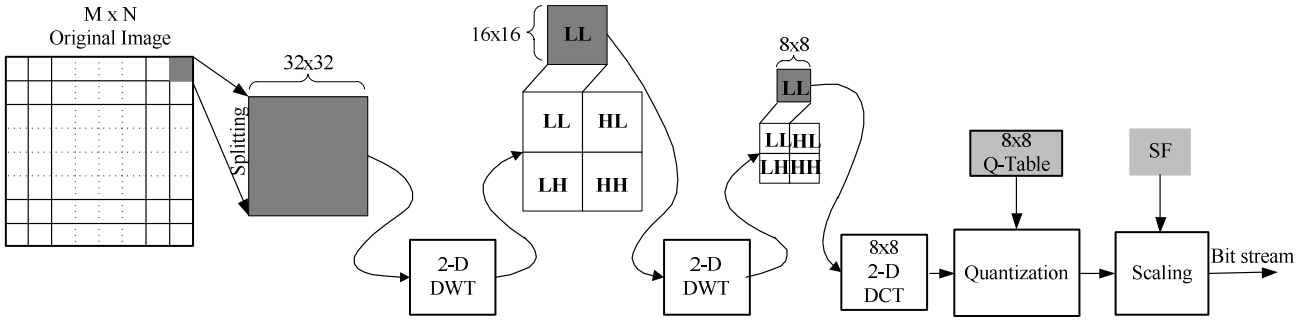

Figure 3.2. Block diagram of the proposed hybrid DWT-DCT algorithm: Compression

3.2.2 The process of data reconstruction

The bit stream after the *SF* is the compressed data of interest. It is rescaled by same *SF* for the reconstruction procedure. Furthermore, the output rescaled data are dequantized by using the same JPEG quantisation table used for the compression procedure. The dequantized data are passed through 2-D inverse DCT. The data obtained after inverse 2-D DCT is then passed through the 2-D inverse DWT at first level. During the 2-D inverse DWT, zero values are padded in place of the detail coefficients. Finally, the output from first level 2-D DWT passed through the 2-D inverse DWT in second level and hence the final image is reconstructed. The entire reconstruction procedure is illustrated in Figure 3.3.

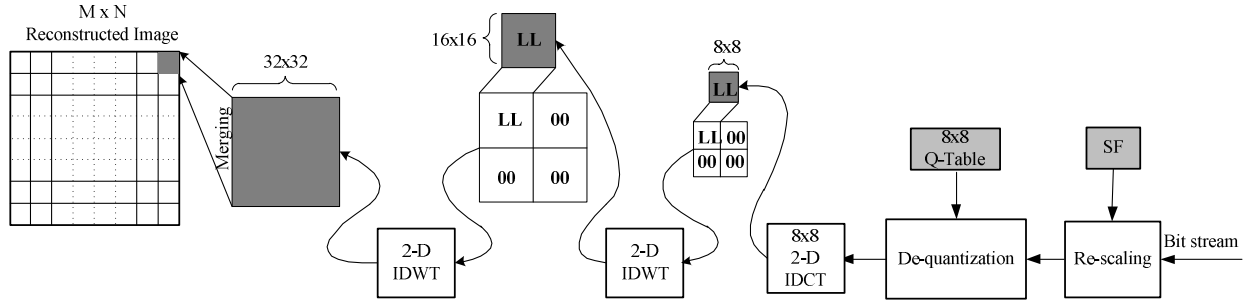

Figure 3.3. Block diagram of the proposed hybrid DWT-DCT algorithm: Reconstruction

Example 3.1: Reconstruction error comparison

A standard image 'Lena' of size 256×256 is taken as example to illustrate the effectiveness of the proposed hybrid algorithm. The image is transformed and reconstructed using proposed hybrid and stand alone DCT, DWT, and FWHT algorithm as well in order to verify the results. The image is compressed at compression ratio (*CR*) of around 96% for all of the three algorithms. The compression ratio is the ratio between discarded data to the original data and is explained in Section 4.2. The absolute error between original image and the reconstructed image using these algorithms for first 500 coefficients taken in progressive order is shown in Figure 3.4. It is clear that the reconstruction error is for the proposed hybrid algorithm is less as compared to the other three stand alone algorithms.

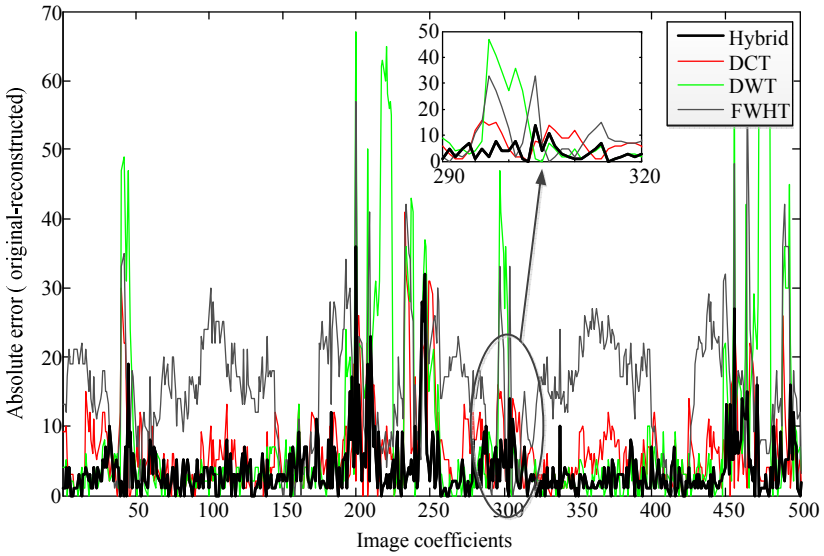

Figure 3.4. Absolute error between original and reconstructed image at 96% compression ratio

In Figure 3.5, (a) is the original image, (b) is the reconstructed image using DCT, (c) is the reconstructed image using DWT (d) is the reconstructed image using WHT, and (e) is the reconstructed image using proposed hybrid algorithm. When the image is reconstructed using standalone DCT, the *PSNR* of this image is 28.66dB. Some blocking artifacts and the contouring effect (around the wall) can be observed in such image. For the image reconstructed using DWT, and FWHT, the *PSNR* is 25.49 dB, and 25 dB respectively. The visual quality of the reconstructed image using DWT and WHT are also worst as compared to others. However, the *PSNR* for the image that is reconstructed using proposed hybrid algorithm is 30.01 dB, which is

quite high than other algorithms. It can also be observed that the image is free from blocking artifacts and the false contouring effect.

(a) Original

(b) *PSNR* = 28.66 dB

(c) *PSNR* = 25.49 dB

(d) *PSNR*= 25 dB

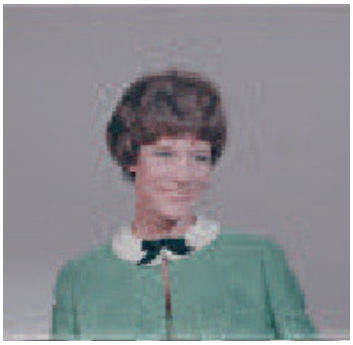

(e) *PSNR*= 30.01 dB

Figure 3.5. Image compression at compression ratio of 96% (a) Original image[1], Reconstructed image using (b) DCT , (c) DWT, (d), FWHT, (e) Hybrid algorithm

[1] Image source: Internet: http://sipi.usc.edu/database/index.html

3.3 Summary

The approach of combining multiple transformations i.e. DWT and DCT has been presented in this chapter. The hybrid algorithm compensated the demerits of standalone DCT and DWT. The proposed algorithm reduced the blocking artifacts that appeared in case of DCT. In standalone DCT, the entire image/frame is divided into 8×8 block in order to apply 8 point DCT. Whereas, in case of hybrid algorithm, image/frame is first divided into 32×32 blocks and two level of DWT is performed for these 32×32 block image. The output after the two level of DWT becomes 8×8 and hence the 8 point DCT is applied for that 8×8 output. This difference in block size causes the blocking artifacts in case of standalone DCT. Similarly, the contouring effect of DCT has also been reduced by using proposed hybrid DWT-DCT algorithm.

CHAPTER 4
PERFORMANCE EVALUATION PARAMETERS

4.1 Introduction

Image compression technique introduces some amount of distortion in the reconstructed image; therefore, evaluation of the image quality is an important issue. The quality of reconstructed images can be evaluated in terms of objective measure and subjective measure. In objective evaluation, statistical properties are considered whereas, in subjective evaluation, viewers see and investigate image directly to determine the image quality [42]. In this chapter, both objective and subjective performance evaluation parameters for image compression algorithm are presented. The objective evaluation measure includes peak signal to noise ratio (*PSNR*), compression ratio (*CR*), variance, and Structural Similarity (*SSIM*) index. Image having same *PSNR* value may have different perceptual quality [43]. The Structural Similarity Metric (*SSIM*) index is another objective measurement technique that is proven to be well matched to perceived visual quality of the image [44]. By adjusting the parameters, tradeoffs can be achieved for compressed image against reconstructed image quality over wide a range. In order to have a visual perception, subjective evaluation of an image/frame has also been conducted for this research work and is also described in this chapter.

4.2 Objective evaluation parameters

The objective quality metric includes the statistical analysis of an input data. There are various objective evaluation parameters. The most commonly used parameters are Peak Signal to Noise Ratio (*PSNR*), Compression ratio (*CR*), variance, and Structural Similarity (*SSIM*) index which are described in the following sub sections.

I. ***Peak Signal to Noise Ratio (PSNR)***

Peak Signal to Noise Ratio (*PSNR*) has been the most popular tool for the objective quality measurement of the compressed image and video. It is simple to compute. The *PSNR* in decibel is evaluated as follows [45]:

$$PSNR = 10 \log_{10} \frac{I^2}{MSE} \tag{4.1}$$

where, I is allowable image pixel intensity level. For 8 bit per pixel image,

$$I = 2^8 - 1 = 255 \tag{4.2}$$

and MSE is the mean square error.

Mean Square Error (MSE): MSE is another important evaluation parameter for measuring the quality of compressed image generally used along with the *PSNR* analysis. It compares the original data and reconstructed data and results the level of distortion. The MSE between the original data and the reconstructed data is:

$$MSE = \frac{1}{MN} \sum_{i=1}^{M} \sum_{j=1}^{N} \left(A_{i,j} - B_{i,j} \right)^2 \tag{4.3}$$

where, A = Original image of size $M \times N$,

B = Reconstructed image of size $M \times N$.

Example 4.1: PSNR comparison

Figure 4.1 shows the standard image 'pepper' of size 512×512. The image is compressed using DCT[1] with two different compression levels to obtain different *PSNR* values. The reconstructed images are shown in Figure 4.1-(b) and (c). The *PSNR* for the image (b) is 26.75 dB, and (c) is 28.55 dB. It is observed that *PSNR* difference between figures (b) and (c) is 1.8 dB. However, when we visualize the reconstructed image, we can observe a reconstruction quality difference between the two reconstructed images. Blocking artifacts is clearly visible in

[1] MATLAB function dct2 has been used.

figure (b). This proves that, *PSNR* is not the sufficient measurement criterion as image is previewed as visual perception. Visual perception at the end level user has been a crucial issue and is growing demand especially in telemedicine, and teleconferencing areas. Hence, it is necessary to take account of both objective measure and subjective measure in order to evaluate the reconstruction quality of compressed data.

(a) Original image (b) *PSNR* = 26.75 dB (c) *PSNR* = 28.55 dB

Figure 4.1. *PSNR* comparison (a) original image[2] and reconstructed image using DCT (b), (c)

II. *Compression Ratio (CR)*

In the process of image compression, it is important to know how much detail (important) coefficient one can discard from the input data in order to preserve critical information of the original data. Compression ratio (*CR*) is a measure of the reduction of the detail coefficient of the data. It can be defined as,

$$CR = \frac{Discarded\ data}{Original\ data} \tag{4.4}$$

The *CR* can be varied to get different image quality. The more the details coefficients are discarded, the higher the *CR* can be achieved. Higher compression ratio means lower reconstruction quality of the image. The quantization table (Q) and the scaling factor (*SF*) are the main controlling parameters of the compression ratio. Each element of the transformed data is divided by corresponding element in the quantization table (Q) and rounded to the nearest integer value. This process makes some of the coefficients to be zero which can be discarded. Furthermore, in order to achieve higher compression ratio, the quantizer output is then divided

[2] Internet: http://sipi.usc.edu/database/index.html

by some scalar constant (*SF*) and rounded to nearest integer value. This process produces more zero coefficients which can be discarded during compression.

Example 4.2: Compression ratio comparison.

(a) Original image (b) *CR* = 85.81 % (c) *CR* = 96.12 %

Figure 4.2. *CR* comparison (a) original image[3] and (b), (c) reconstructed image using 2-D DCT

In Figure 4.2, the original image of monarch of size 256×256 is presented. Figure 4.2-(a) is original image and Figure 4.2(b) and Figure 4.2(c) are reconstructed image using DCT[4] at two different compression ratio. When the image is compressed at 85.81 % of compression ratio as shown in Figure 4.2(b), the reconstruction looks visually similar to the original one. However, when the compression ratio is increased to 96.12 % as shown in Figure 4.2-(c), the visible distortion is evident. This clearly shows that the overall quality of reconstruction depends on the compression ratio.

III. ***Variance***

Variance is another tool to calculate the performance of image compression algorithm. Variance describes how far certain value deviates from the mean. It's the measure of variability from an average. In signal processing, the variances, σ_k^2 (k=1, 2…N), are represented by the Eigen values of the transformed coefficient [46]. N is the size of input data block. The lower the variance, higher will be the energy compaction property. The energy compaction property

[3] Image source: Internet: http://sipi.usc.edu/database/index.html
[4] MATLAB function dct2 has been used.

defines that most of the information signal tends to concentrate in the low frequency component. Higher the energy compaction property, the better is the compression algorithm.

Example 4.3: Variance calculation.

Any random sequence $u(n)$ is called $Markov - p$, or p^{th} order Markov, if the conditional probability of $u(n)$ given the entire past is equal to the conditional probability of $u(n)$ given only $u(n-1), \dots u(n-p)$ [47].

$$Prob[u(n)|u(n-1), u(n-2), \dots] = Prob[u(n)|u(n-1), \dots., u(n-p)], \quad \forall n \tag{4.5}$$

The covariance function of first order stationary Markov sequence $u(n)$ is given as

$$r(n) = \rho^{|n|}, \qquad \forall n \tag{4.6}$$

For first order Markov sequence having the correlation matrix of size N and correlation coefficient, ρ, the correlation matrix R is as given below [47]

$$R = \begin{bmatrix} 1 & \rho & \rho^2 & . & . & . & \rho^{N-1} \\ \rho & 1 & . & . & . & . & . \\ . & . & . & . & . & . & . \\ . & . & . & . & . & . & . \\ . & . & . & . & . & . & \rho^2 \\ . & . & . & . & . & . & \rho \\ \rho^{N-1} & . & . & . & . & \rho & 1 \end{bmatrix} \tag{4.7}$$

For $N = 8$ and $\rho = 0.95$, the correlation matrix R is as shown below:

$$R = \begin{bmatrix} 1 & 0.95 & 0.90 & 0.85 & 0.81 & 0.77 & 0.73 & 0.69 \\ 0.95 & 1 & 0.95 & 0.90 & 0.85 & 0.81 & 0.77 & 0.73 \\ 0.90 & 0.95 & 1 & 0.95 & 0.90 & 0.85 & 0.81 & 0.77 \\ 0.85 & 0.90 & 0.95 & 1 & 0.95 & 0.90 & 0.85 & 0.81 \\ 0.81 & 0.85 & 0.90 & 0.95 & 1 & 0.95 & 0.90 & 0.85 \\ 0.77 & 0.81 & 0.85 & 0.90 & 0.95 & 1 & 0.95 & 0.90 \\ 0.73 & 0.77 & 0.81 & 0.85 & 0.90 & 0.95 & 1 & 0.95 \\ 0.69 & 0.73 & 0.77 & 0.81 & 0.85 & 0.90 & 0.95 & 1 \end{bmatrix} \tag{4.8}$$

The above Markov sequence is considered as input and transformed using DCT. The corresponding transformed coefficient is shown in Figure 4.3.

7.02494	0	-0.1868	0	-0.042	0	-0.0133	0
0	0.57491	0	-0.0093	0	-0.0028	0	-0.0007
-0.1868	0	0.17333	0	-0.0002	0	-8E-05	0
0	-0.0093	0	0.08196	0	-0.0003	0	-7E-05
-0.042	0	-0.0002	0	0.05119	0	-2E-05	0
0	-0.0028	0	-0.0003	0	0.03699	0	-2E-05
-0.0133	0	-8E-05	0	-2E-05	0	0.03003	0
0	-0.0007	0	-7E-05	0	-2E-05	0	0.02665

Figure 4.3. Transformed coefficient of Markov sequence using DCT

Now the, variance of the transformed coefficient can be obtained as the Eigen value of the above transformed coefficient as shown below.

$$\sigma^2 = [7.030 \quad 0.575 \quad 0.168 \quad 0.082 \quad 0.051 \quad 0.037 \quad 0.030 \quad 0.027]$$

IV. ***Structural Similarity (SSIM) Index***

The main paradigm of *SSIM* is based on the assumption that the image signals are highly structured, i.e. the neighbouring pixels of the image signals are highly correlated. This correlation carries important information about the structure of the image in the visual perception [48]. Therefore, *SSIM* provides a good approximation to the perceived image quality. During the data compression, the structures of the reconstructed data are distorted. This distortion can be analyzed using *SSIM* index defined as below [44]:

$$SSIM(A,B) = \frac{(2\mu_A\mu_B + C_1)\ (2\sigma_{AB} + C_2)}{(\mu_A^2 + \mu_B^2 + C_1)\ (\sigma_A^2 + \sigma_B^2 + C_2)} \tag{4.9}$$

where,

μ_A, μ_B = mean intensities of original data A and reconstructed data B;

σ_A, σ_B = standard deviation of original data A and reconstructed data B;

C_1, C_2 = constant. The standard value of C_1 and C_2 are 0.01 and 0.03 respectively [44].

The mean intensity can be calculated as below.

$$\mu = \frac{1}{N}\sum_{i=1}^{N} x_i \tag{4.10}$$

The standard deviation is mathematically represented as:

$$\sigma = \sqrt{\frac{1}{N}\sum_{i=1}^{N}(x_i - \mu)^2} \tag{4.11}$$

and,

$$\sigma_{AB} = \frac{1}{N-1}\sum_{i=1}^{N}(A_i - \mu_A)(B_i - \mu_B) \tag{4.12}$$

If the reconstructed data is exactly similar to original data then the best *SSIM* index of unity can be achieved.

4.3 Subjective evaluation parameter

For the end user, the visual perception of the reconstructed image is essential. In some cases the objective quality assessment does not give proper information about the quality of the reconstructed image. In such scenarios, it is important to analyse the reconstructed image using subjective analysis. When the subjective measure is considered, viewers focus on the difference between reconstructed and original image and correlates the differences.

Example 4.4: Human visual perception.

In Figure 4.4, a standard image of parrot having size of 512×512 is considered for demonstration. The image is compressed using proposed, DCT, and DWT algorithm at the compression ratio of 96 %. The respective *PSNR* values in dB are shown in Figure 4.5.

(a) (b)

(c) (d)

Figure 4.4. Visual perception of (a) original image[5] and reconstructed images using (b) proposed (c) DCT, and (d) DWT.

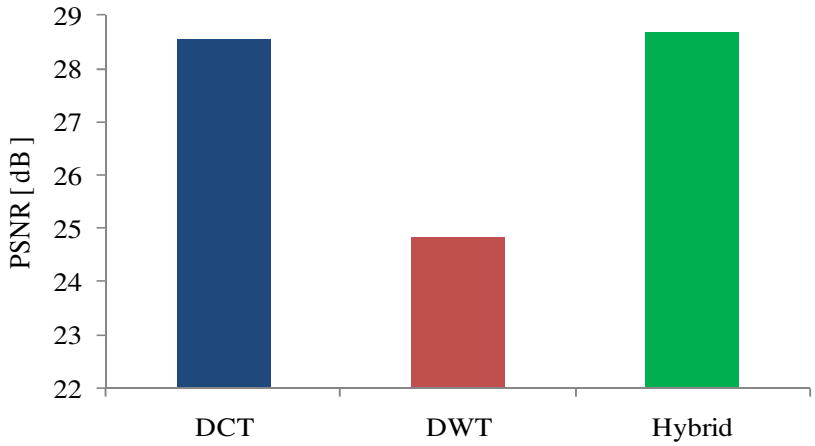

Figure 4.5. *PSNR* of DCT, DWT and proposed hybrid DWT-DCT

[5] http://r0k.us/graphics/kodak/kodim23.html

From Figure 4.5, it is clear that the *PSNR* value for DCT algorithm is 28.55 dB, for proposed hybrid DWT-DCT algorithm is 28.69 dB which is slightly higher than that of DCT. However, if we visually analyse the reconstructed image (Figure 4.4), it is clear that, the DCT has contour effect in its reconstructed image. The image reconstructed using proposed hybrid algorithm has better visual quality as compared to the reconstructed image obtained using DCT as well as DWT.

4.4 Summary

In this chapter, the objective and subjective evaluation parameter generally used for image compression analysis has been presented. For the objective evaluation *PSNR*, *CR*, *SSIM* index, and variance have been discussed. These all metrics are simple to compute and shows the statistical properties of reconstructed data. However, in some cases, this parameter may not exactly define the visual reconstruction quality. Thus, subjective evaluation parameter has also been discussed for the reconstruction quality analysis.

CHAPTER 5
SIMULATION RESULTS: A PERFORMANCE EVALUATION

5.1 Introduction

This section evaluates the performance of the proposed hybrid DWT-DCT algorithm. The proposed hybrid algorithm is applied on several types of images: natural images, medical images, benchmark images such that the performance of proposed algorithm can be verified for various applications. The proposed algorithm is also verified using Markov sequence. The reconstructions of the images are also reported. The natural images are captured by a Nikon D40X Digital Single Lens Reflex (DSLR) camera in raw format. The medical images include endoscopic images of different parts of Gastro Intestinal (GI) tract and some x-ray images. All these medical images are obtained from [49]. These benchmark images are the standard image generally used for the image processing applications and are obtained from [50]. The types of images are categorized in Table 5.1.All these sample images are shown in Appendix.

Table 5.1 Types of images used for study

Image type	
Type 1	Natural images [captured by Nikon D40X]
Type 2	Medical images [49]
Type 3	Bench mark images[50]

Furthermore, the algorithm is also applied on several video sequences, such as, endoscopic videos, Quarter Common Intermediate Format (QCIF) videos, and High Definition (HD) videos. The endoscopic videos show various parts of the intestine. The endoscopic videos are obtained from [51]. There are four different types of QCIF videos considered: ‘Akiyo’, ‘Bridge’, ‘Silent’, and ‘Suzie’. Similarly, four HD video sequences e.g., ‘Stockholm’, ‘Shield’, ‘Ice’, and ‘City’ have been considered. The types of video samples are tabulated in Table 5.2. All these QCIF

videos and HD videos are standard videos generally used in video processing studies. These videos are obtained from [52]. The results of the exhaustive simulation for all images and videos are presented in this section. The results are compared with the JPEG-based DCT, Daubechies-based DWT, and the WHT algorithms.

Table 5.2 Types of videos used for study

Video type	
Type 1	Endoscopic video [51]
Type 2	QCIF video [52]
Type 3	HD video [52]

5.2 Simulation tool

The algorithm was implemented in MATLAB simulation tool. For the DWT and DCT, MATLAB functions "dwt2" and "dct2" has been considered, respectively. The evaluation parameters (PSNR, CR, SSIM index, and Variance), sub-sampling, quantization and scaling routines were manually programmed in MATLAB.

For a better assessment, the following approach has been adopted:

i. The *PSNR* is evaluated for a constant *CR*. While evaluating the *PSNR*, highest *CR* is intended to achieve by using the scaling factor without visually distorting the reconstructed image.

ii. The average *PSNR* is determined and the *CR* is computed for that particular *PSNR*.

iii. The *SSIM* is computed for the initial constant average *CR*.

iv. The proposed algorithm is compared with DCT, DWT and FWHT algorithms.

5.3 Performance evaluation: Images

In this section, the performance evaluation parameters for images tabulated in Table 5.1 are presented. All the images are compressed, and then reconstructed using the JPEG-based

DCT, the Daubechies-based DWT, and the proposed hybrid DWT-DCT algorithm. Furthermore, in order to verify the effectiveness of the proposed algorithm, it is also compared with FWHT.

5.3.1 Natural image

Natural images are taken by Nikon D40X DSLR camera in raw format. Ten random images of books, plants, landscape, buildings and texture are taken for the analysis. Figure 5.1 shows the *PSNR* values obtained for the natural images at a constant *CR* of around 96 % in case of DCT, DWT and proposed algorithm. In case of FWHT, the resulting *PSNR* value is very low (in the range of 7~15 dB) and the image reconstruction looks worst visually at higher *CR* as 96 %. Hence, it is compared at around 87 % of *CR*. It is clear that, the proposed hybrid algorithm has higher *PSNR* compared to DCT, FWHT and DWT algorithms. It is also clearly observed that FWHT has the least *PSNR* (less than 20 dB in average) even though it is compared only at *CR* of 87 %. The image number 3, 6, 8, and 10 are gradient images and they consist of dark colours such as red, green, and black. It is observed that for these images, the hybrid algorithm has the highest *PSNR* and outperforms the other three algorithms by a good margin.

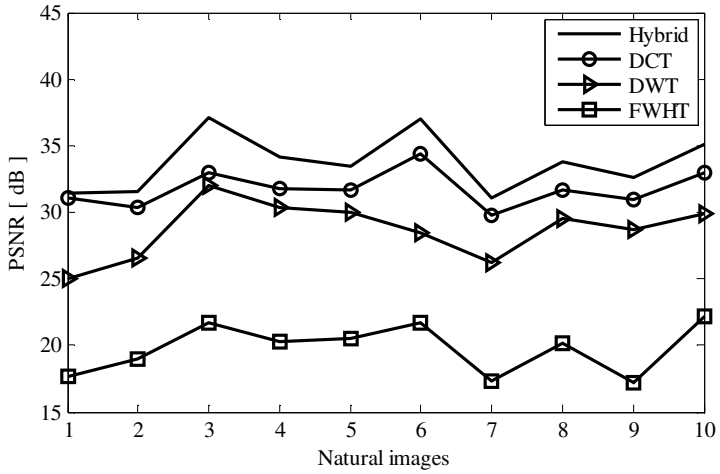

Figure 5.1. *PSNR* for type 1 images for average compression ratio of 96%

The typical value for image compression ranges from 20 ~ 40 dB [32, 53, 54]. The compression ratio comparison at the constant *PSNR* should lie within the above range. Since the *PSNR* value for the FWHT is less than 20 dB in average at 87% of compression ratio (Figure 5.1), it is not considered for the compression ratio comparison studies for all types of images and videos presented in this thesis work.

Since this research work is based on high compression ratio, the next algorithm having least *PSNR* is DWT algorithm. The average *PSNR* for the DWT is around 28dB. In order to achieve same *PSNR* for the proposed and DCT algorithms, the *CR* of these two algorithms has to be decreased. Figure 5.2 shows the *CR* of different algorithm for a fixed *PSNR* of around 28dB. It can be seen that the *CR* obtained by proposed algorithm is higher compared to other algorithms. In case of the DWT, since the compression depends only on the number of level of decomposition, the *CR* stays as constant in Figure 5.2.

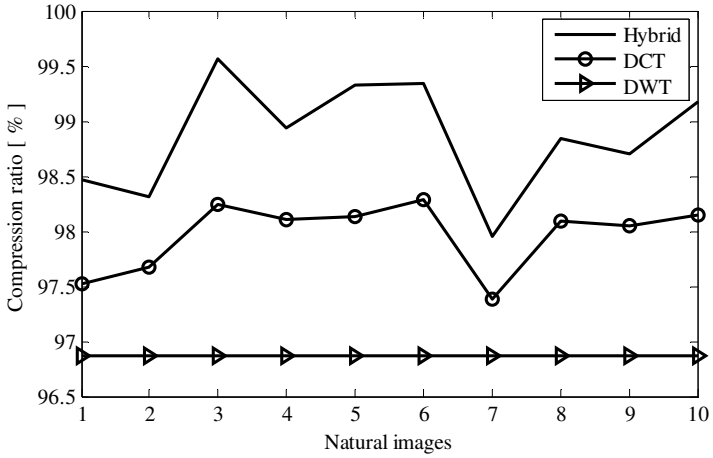

Figure 5.2. Compression ratio for type 1 images for average *PSNR* of 28 dB

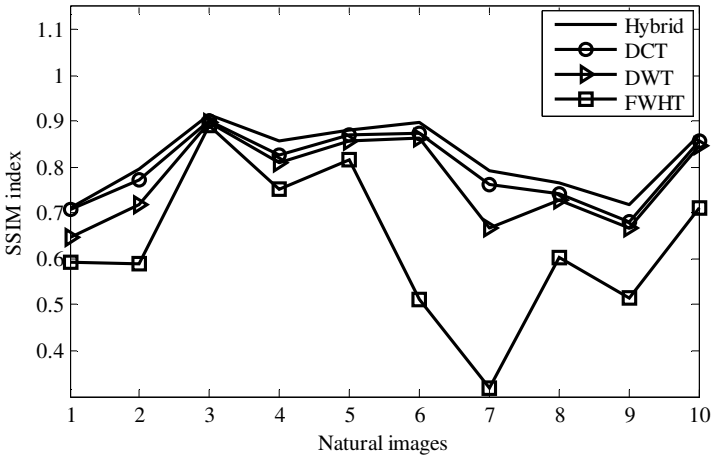

Figure 5.3. *SSIM* index for type 1 images for average compression ratio of 96%

Similarly, the *SSIM* index for type 1 images are calculated for DCT, DWT and proposed algorithm at *CR* around 96 % and for FWHT algorithm at around 87 % and plotted in Figure 5.3. It is observed that for this constant *CR*, the *SSIM* index is higher for the hybrid DWT-DCT scheme.

The original and reconstructed images for image number 1 of the type 1 image are shown in Figure 5.4. The *PSNR* values for reconstructed image using, DCT, DWT, FWHT, and hybrid algorithm are 31dB, 25 dB, 23.48 dB, and 31.8 dB respectively. The FWHT has very low *PSNR* as compared to other algorithms in this case, and hence the reconstruction quality is least. Therefore, visual illustration of the reconstruction quality of the FWHT has been discarded for all types of images and videos in this thesis work. The false contouring effect is clearly visible in the image reconstructed by the DCT and it is due to the high compression ratio. However, the reconstructed image obtained using proposed algorithm is free from contouring effect even though the *PSNR* difference between DCT and proposed algorithm is only 0.8 dB.

5.3.2 Medical image

In this sub section, the medical images are used to verify the efficiency of the proposed hybrid algorithm and are compared with stand alone DCT, DWT, and WHT algorithm. The medical images in raw form are difficult to obtain and hence, already compressed medical images in JPEG format are downloaded from source [49] are considered for the analysis. Sixteen different medical images are considered for the analysis. The image number 1 to10 are endoscopic images and 11 to 16 are x-ray images.

In Figure 5.5, PSNR values computed at constant compression ratio of around 96% are compared for DCT, DWT and proposed hybrid algorithms and around 87% for the WHT. Previous research on image compression suggests the acceptable PSNR for medical images should be equal or greater than 35 dB [55, 56]. It is observed from Figure 5.5 that, even for very high CR of around 96%, the PSNR value for the proposed algorithm is higher than 35dB – this satisfies the acceptability of the proposed scheme for the compression of medical images. Furthermore, it is also observed that images 1, 5, and 9 have sharp increase in the PSNR value. The main reason behind it is that these images are bright in colour, and have fine details and textures. On the other hand, the images 3 and 10 have sharp decrease in the PSNR value. This is due to the fact that these images have sharp transitions and edges. In addition, these images are less bright than the other images.

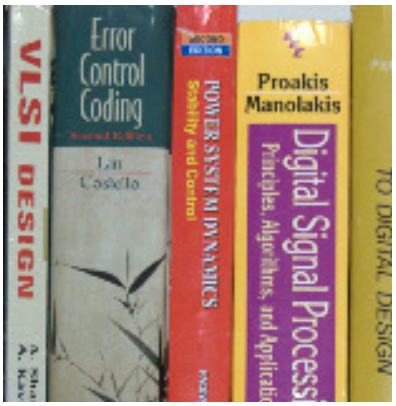

(a) Original image

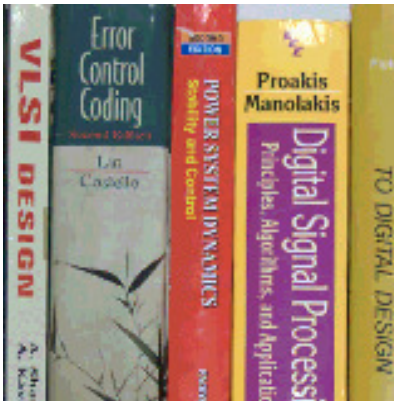

(b) *PSNR* = 31 dB

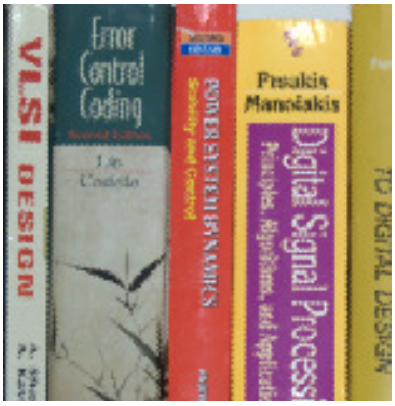

(c) *PSNR* = 25 dB

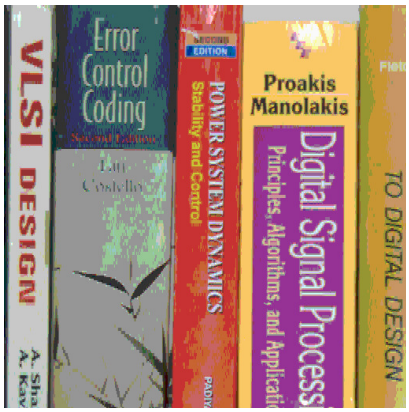

(d) *PSNR* = 23.48 dB

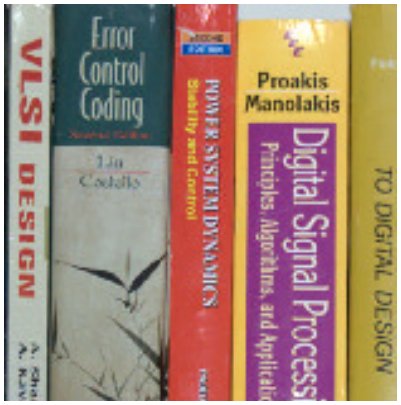

(e) *PSNR* = 31.8 dB

Figure 5.4. (a) Original (image no. 1, type 1), reconstructed image using (b) DCT, (c) DWT, (d) FWHT (e) Hybrid DWT-DCT

It is also observed that for specific compression ratio, PSNR using proposed hybrid algorithm outperforms the DCT, FWHT, and DWT algorithms.

In Figure 5.5, since the average PSNR for the DWT is around 32 dB, different studies are carried out for the variation in the CR at that particular PSNR of 32 dB. The resulting plot is shown in Figure 5.6 which is consistent to the results of Figure 5.2. It is clearly observed that proposed hybrid algorithm has achieved highest compression ratio as compared to other two algorithms at a given constant PNSR.

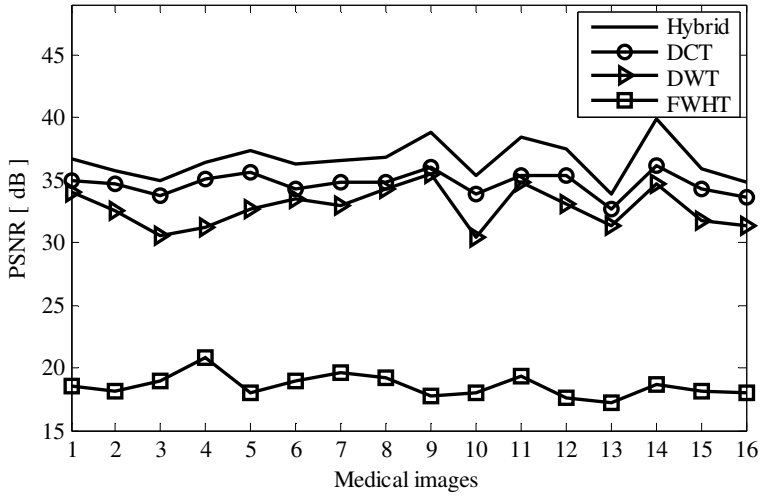

Figure 5.5. *PSNR* for type 2 images for average compression ratio of 96%

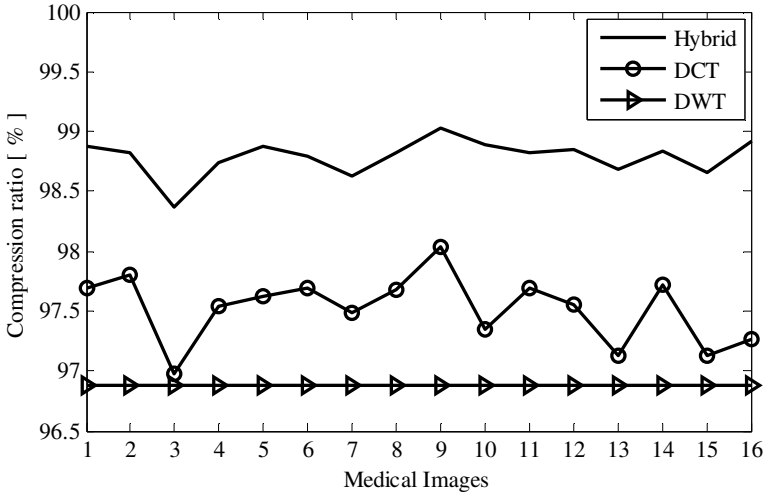

Figure 5.6. Compression ratio for type 2 images for average *PSNR* of 32 dB

Figure 5.7 shows the comparison plots of *SSIM* index of the medical images for constant *CR* of 96 % in case of DCT, DWT and proposed algorithm. For FWHT algorithm, the *SSIM* index comparison is analyzed at constant compression ratio of 87 %. It is observed that the value of *SSIM* index using the proposed hybrid algorithm has highest value. The range of *SSIM* index for endoscopic image is from 0.45 – 0.85, whereas for X-ray images, the value of *SSIM* index is between 0.75-0.95, which shows a good perceptual quality.

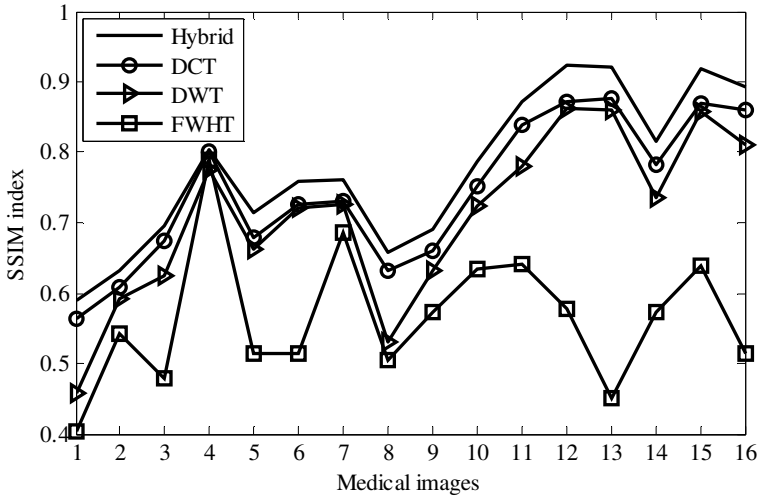

Figure 5.7. *SSIM* index for type 2 images for average compression ratio of 96%

The original and reconstructed images for image number 2 of the type 2 image are shown in Figure 5.8. The *PSNR* value for DCT, DWT and proposed algorithm is 31 dB, 29 dB, and 36.5 dB respectively. It is visually observed that the DCT algorithm has encountered blocking effect as well as false contouring effect. The image reconstructed using DWT algorithm has least PSNR value and is also unreadable. From this visible illustration, it is evident that proposed hybrid algorithm has better reconstruction quality.

5.3.3 Benchmark image

In this subsection, the proposed hybrid algorithm is tested on some benchmark images. Five bench mark images ‘house’, ‘jelly beans’, ‘couple’, ‘girl1’ and ‘girl2’ from source [50] are considered for the analysis. Figure 5.9 shows the plot of *PSNR* for five different types of benchmark images at a constant *CR* of 96% for DCT, DWT and proposed algorithm. For FWHT algorithm the *PSNR* is analysed at constant compression ratio of 87 %.

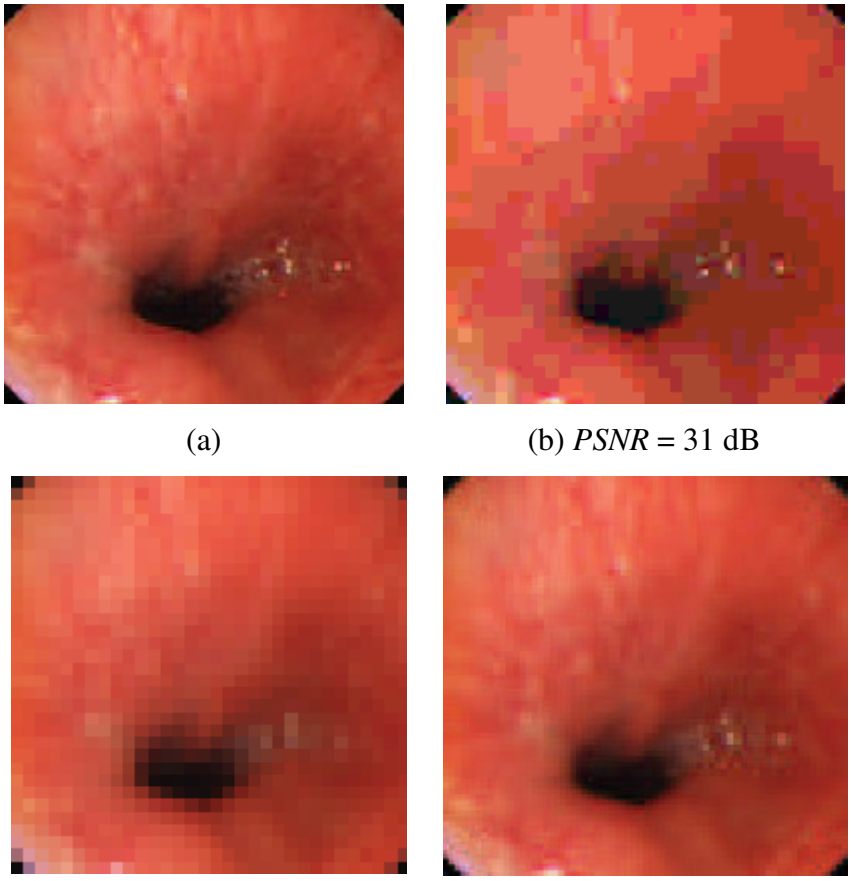

(a) (b) *PSNR* = 31 dB

(c) *PSNR* = 29 dB (d) *PSNR*= 36.5 dB

Figure 5.8. (a) Original (image no.2, type 2), reconstructed image using (b) DCT, (c) DWT, (d) Hybrid DWT-DCT

From Figure 5.9, it is seen that in the case of the hybrid algorithm, the image number 2 and 5 have *PSNR* of around 29 dB, whereas for other images the *PSNR* is only between 25 to 26 dB. This is due to the fact that the image number 2 and 5 consist fine details and texture of gradually changing colour and the image number 1, 3, and 4 are less bright and have sharp transitions. It is observed that the hybrid algorithm performs better for the gradient images having fine details. All benchmark images in this study have higher *PSNR* when they are compressed using proposed hybrid DWT-DCT algorithm.

Figure 5.10 shows the plot of variation in *CR* for the average *PSNR* of 25dB. The results are consistent with previous results (Figure 5.2 and Figure 5.6). The proposed hybrid DWT-DCT algorithm has the higher compression ratio as compared to stand alone DCT and DWT algorithm.

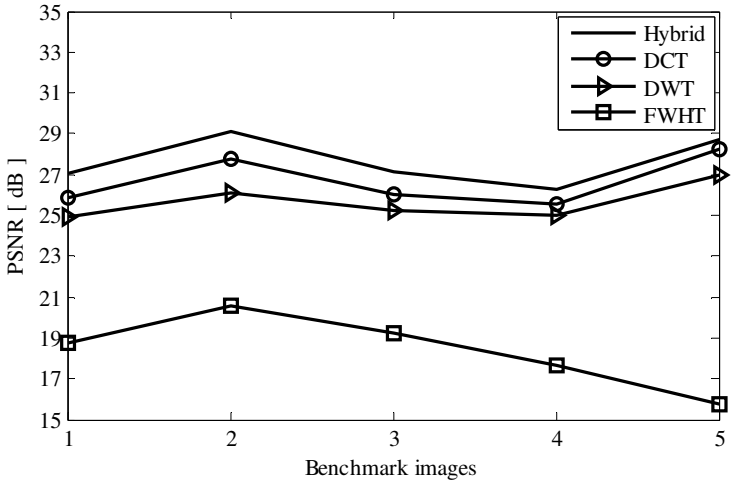

Figure 5.9. *PSNR* for type 3 images for average compression ratio of 96 %

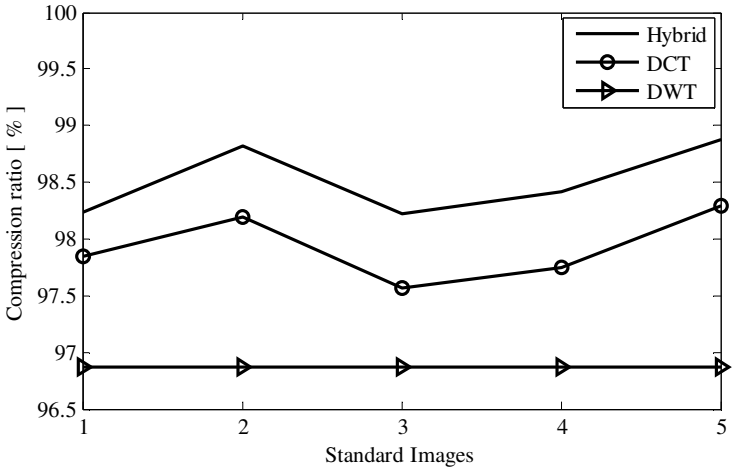

Figure 5.10. Compression ratio for type 3 images for average *PSNR* of 25 dB

The *SSIM* index for benchmark images at constant *CR* of 96 % for DCT, DWT and proposed algorithm is illustrated in Figure 5.11. For the FWHT, the *PSNR* is compared at constant *CR* of 87 %. It is observed that the proposed algorithm has higher *SSIM* index compared to other three algorithms.

The original and reconstructed images for image number 1 of the type 3 image are shown in Figure 5.12. The *PSNR* values for DCT, DWT and proposed hybrid algorithm are 25.98 dB, 23.42 dB, and 30.41 dB respectively. As in the previous case, the false contouring effect is visible in the image reconstructed by the DCT algorithm. The image reconstructed using DWT algorithm is also very poor compared to the one with the proposed hybrid algorithm.

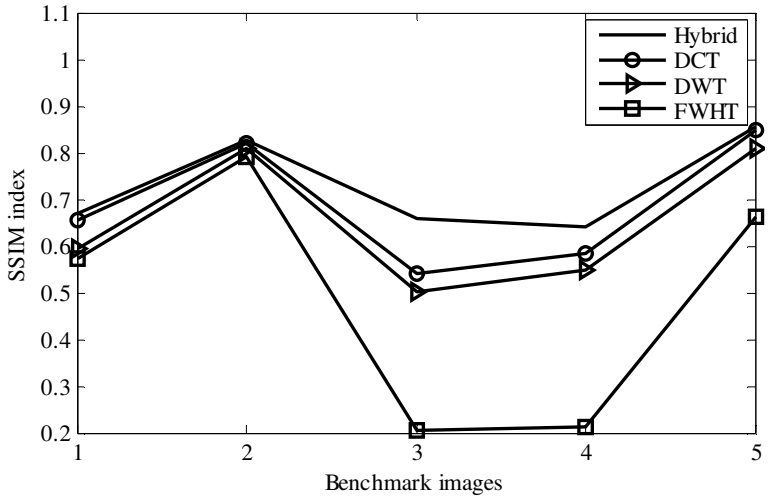

Figure 5.11. *SSIM* index for type 3 images for average compression ratio of 96 %

(a) Original image

(b) *PSNR* = 25.98 dB

(c) *PSNR* = 23.42 dB

(d) *PSNR*= 30.41 dB

Figure 5.12. (a) Original, reconstructed image using (b) DCT, (c) DWT, (d) Hybrid DWT-DCT

5.4 Performance evaluation: Videos

In order to demonstrate the performance advantage of video signals, the hybrid DWT-DCT algorithm has been applied to several video clips: endoscopic video, QCIF video, and HD video as tabulated in Table 5.2. The proposed algorithm has been applied to spatial domain only, i.e., the video is treated as series of still frames.

5.4.1 Endoscopic video

All of the endoscopic videos are taken from the source [51]. At first, single endoscopic video is analyzed. Since the endoscopic video has consistent image frames, only 30 frames of a video are considered. It is observed that performance of the FWHT algorithm is least as compared to other standalone DCT and DWT and proposed algorithm and the *PSNR* value is less than 20 dB in average for all types of images for 87 % compression ratio in the section 0. Hence in this section, the performance of the FWHT algorithm is not considered for the analysis

Figure 5.13 reveals the *PSNR* for all three algorithms for 30 frame of an endoscopic video at a very high compression ratio, 98%. It can be seen that at such high *CR*, the *PSNR* achieved by the hybrid and the DCT algorithm are very close. As described earlier, the DWT has a constant *CR* due to constant level of decomposition.

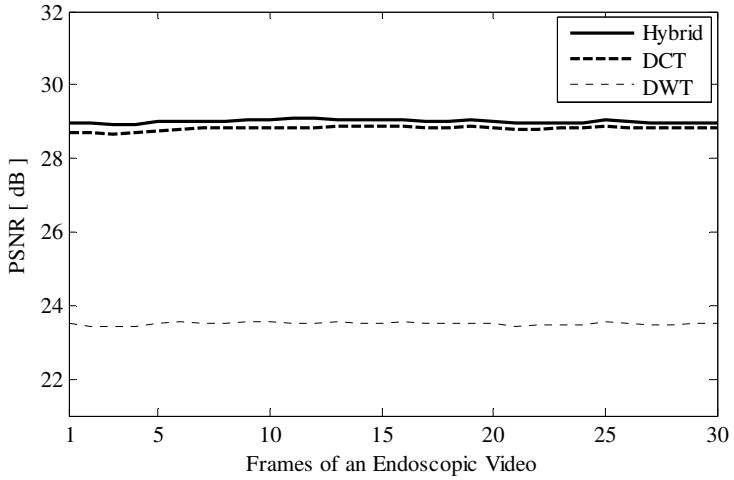

Figure 5.13. *PSNR* for different frames of type 1 video for average compression ratio of 98%

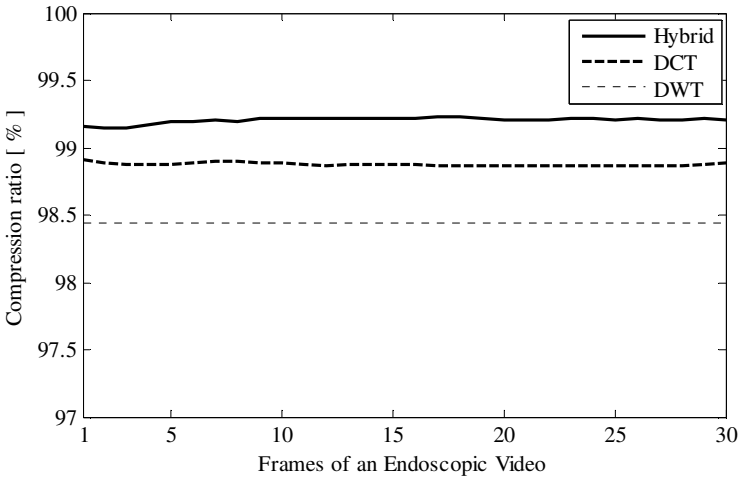

Figure 5.14. Compression ratio for different frames of type 1 video for average *PSNR* of 23.5 dB

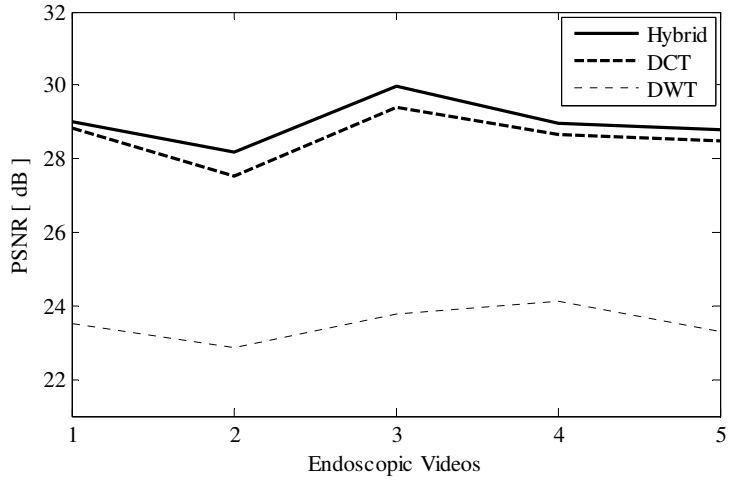

Figure 5.15. Average *PSNR* for type 1 videos for average compression ratio of 98%

Figure 5.14 shows the *CR* of three algorithms for the same frames at an average *PSNR* of 23.5 dB. The reason behind taking average *PSNR* of 23.5 dB is that the minimum average *PSNR* of the DWT is around 23.5 dB. Hence, for a better comparison of variation in the *CR*, the *PSNR* for both the DCT and the hybrid schemes are adjusted to be at around 23.5 dB. From Figure 5.14, we can see that hybrid algorithm has the highest *CR* (around 99.2%).

In order to further verify the algorithm, in the next step, the algorithm is applied on the first 30 frames of five individual endoscopic videos. The *PSNR* values for three algorithms are calculated and the average value of *PSNR* of 30 frames is taken consideration. Figure 5.15 shows the *PSNR* value for three algorithms at constant average compression ratio of 98 %.

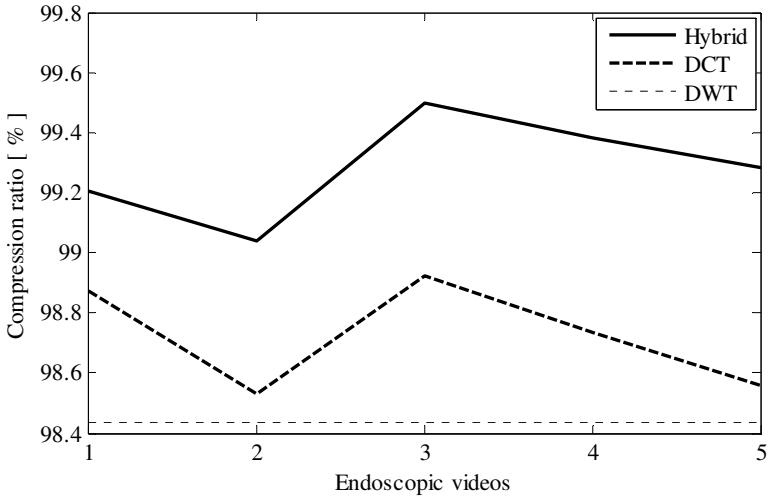

Figure 5.16. Average compression ratio for type 1 video for average *PSNR* of 23.5 dB

Similarly, for constant average *PSNR* of 23.5 dB, the compression ratios of 30 frames of each five videos are calculated. The average value of compression ratio of 30 frames is calculated and has been plotted in Figure 5.16. These results are consistent with the previous results obtained for the images. The performance of the DWT-DCT based hybrid approach is proved to be better than the other two stand alone algorithm.

Visual illustration of the proposed algorithm for first frame of endoscopic video (no. 1) along with other reconstructed frames using three algorithms is shown in Figure 5.17. The *PSNR* values for DCT, DWT, and proposed algorithm are 27.94 dB, 23.49 dB, and 28.98 dB respectively. The false contouring effect due to extreme compression (i.e., 98%) is clearly visible in the frame reconstructed using the JPEG-based DCT. Similarly, it is observed that the reconstructed frame using DWT contains some noises and has least *PSNR* value. It is also seen that the proposed hybrid algorithm has higher *PSNR*. It can also be depicted that proposed hybrid DWT-DCT algorithm shows better reconstruction quality and also free form false contouring effect.

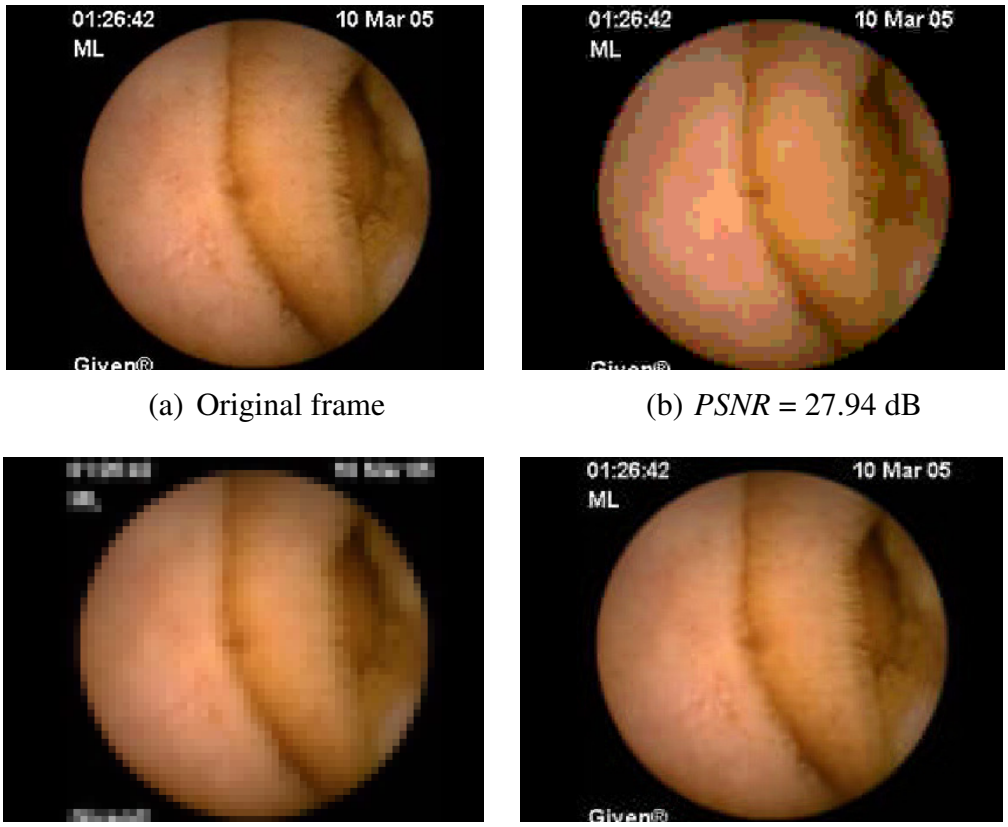

(a) Original frame (b) *PSNR* = 27.94 dB

(c) *PSNR* = 23.49 dB (d) *PSNR*= 28.98 dB

Figure 5.17. (a) Original (first frame of endoscopic video no. 1), reconstructed image using (b) DCT, (c) DWT, (d) Hybrid DWT-DCT

5.4.2 QCIF videos

For further analysis, in this sub section QCIF videos are considered. The QCIF videos are Quarter Common Intermediate Format videos of size 176×144 and generally used for video conferencing applications. There are several standard QCIF videos for video processing studies [52]. Among them, four QCIF videos: 'Akiyo', 'Bridge', 'Silent', and 'Suzie' are considered for the analysis. Initially, a QCIF video 'Akiyo' is taken for the analysis.

Figure 5.18 shows the *PSNR* computed at an average *CR* of 96% for 90 frames of the video sequence. It is observed that proposed hybrid algorithm show higher *PSNR* compared to other two algorithms.

The DWT algorithm has least average *PSNR* of around 24 dB. Therefore, the *CR* analysis is performed at *PSNR* of 24 dB as shown in Figure 5.19. Yet again, the proposed hybrid algorithm shows the better performance and consistent result.

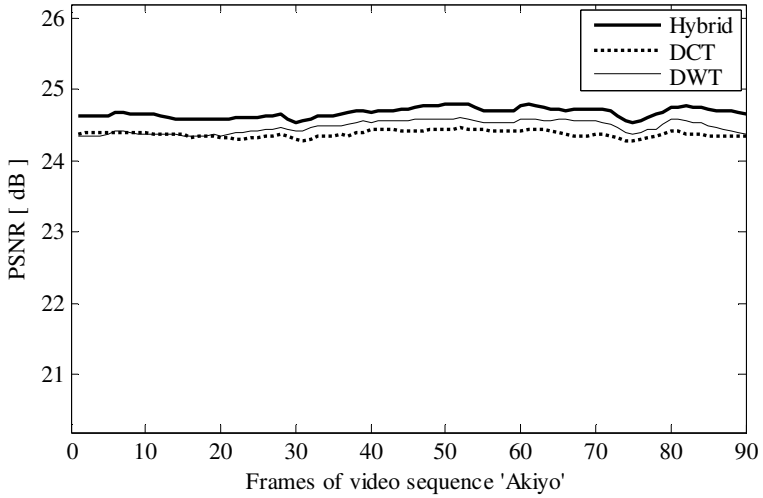

Figure 5.18. *PSNR* for different frames of type 2 video for average compression ratio of 96 %

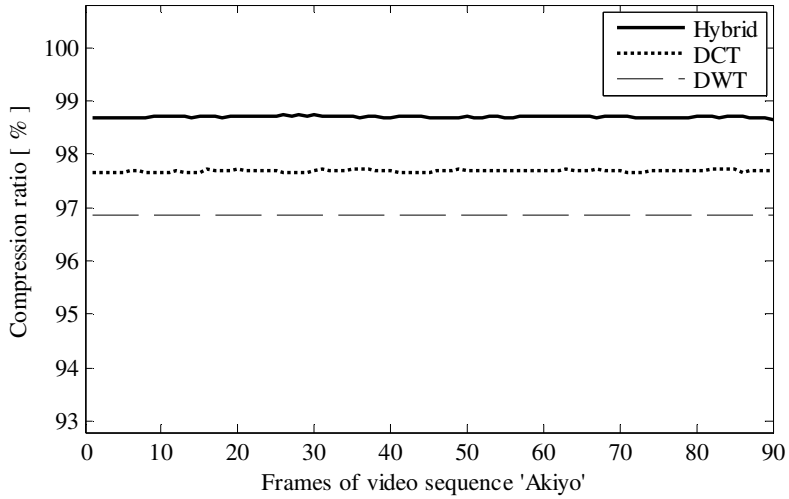

Figure 5.19. Compression ratio for different frames of type 2 video for average *PSNR* of 24 dB

The *SSIM* index versus frames of Akiyo QCIF video for DCT, DWT and proposed algorithm at constant *CR* of 96 % is shown in Figure 5.20. The *PSNR* value obtained using DCT, DWT and proposed hybrid algorithm are 27.94 dB, 23.49 dB, and 28.98 dB respectively. It is

clearly observed that he hybrid algorithm better *PSNR* than the DCT, DWT and FWHT algorithm. The contouring effect due to the high compression ratio is clearly visible in case of DCT algorithm.

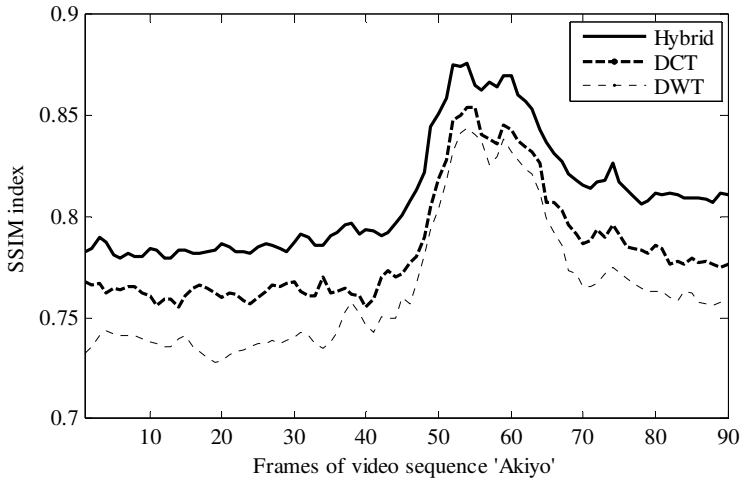

Figure 5.20. *SSIM* index for different frames of type 2 video for average *CR* of 96 %

Subsequently, for the further verification of the algorithm, the analysis is performed for four QCIF videos. The 'Akiyo' and 'Silent' sequences are the news reading shows. In these video sequences, the object is moving while the background is still. The 'bridge' sequence is the view of bridge with no motion of camera. The background is almost constant and has object in motion. The sequence 'Suzie' is the video of lady talking on phone and taken in a close-up; the object is also moving very fast.

In Figure 5.21, the performance of three algorithms for four QCIF videos with respect to *PSNR* for an average *CR* of 96% is presented. All the *PSNR* values are calculated for 90 frames and average value is plotted. It is depicted that the hybrid algorithm performs best for the video sequence with more details and moving objects (such as, 'Suzie'). It is also observed that hybrid scheme consistently outperforms the JPEG-based DCT and the DWT schemes.

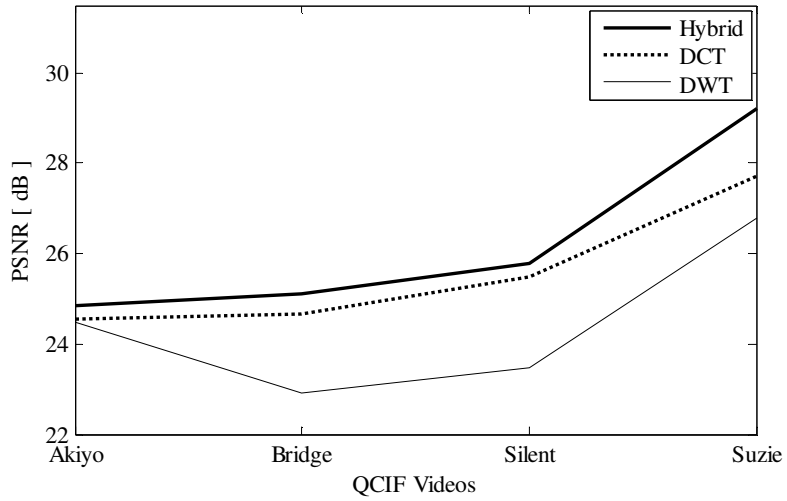

Figure 5.21. Average *PSNR* for 4 different type 2 videos for average compression ratio of 96%

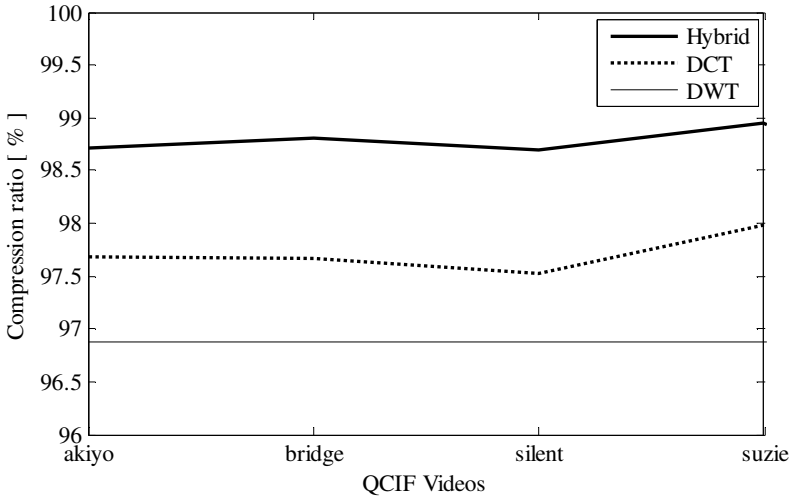

Figure 5.22. Average compression ratio for 4 different type 2 videos for average *PSNR* of 24 dB

Figure 5.22 shows the performance evaluation with respect to *CR* at constant average *PSNR* of 24 dB. Once again, it is seen that when the *PSNR* of the hybrid and the DCT algorithms are equal to that DWT, the hybrid algorithm results the highest *CR*. It is also observed that the results are consistent for all video sequences.

Figure 5.23 shows the first frame of 'Suzie' along with other reconstructed frames using three schemes. The blocking artifact is visible in case of DCT. It can also be seen that DWT performs the least. The proposed hybrid algorithm has the highest *PSNR* and better reconstruction quality as compared to other two stand alone DCT and DWT algorithms.

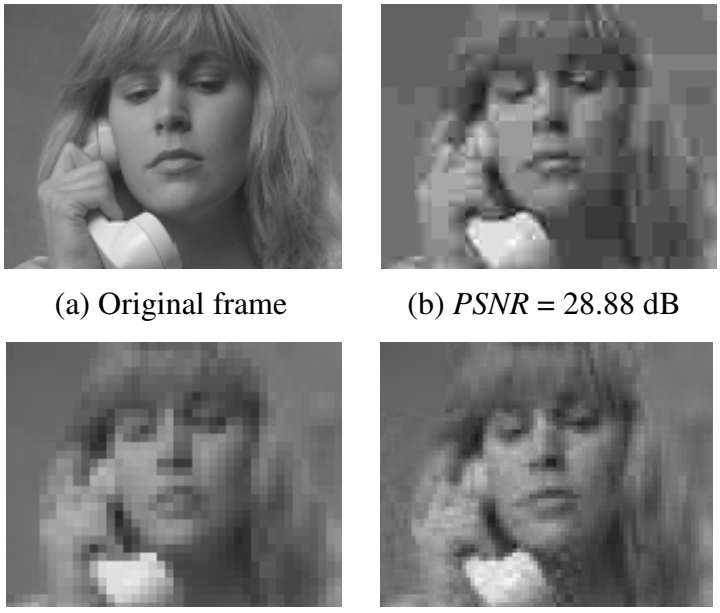

(a) Original frame (b) *PSNR* = 28.88 dB

(c) *PSNR* = 27.57 dB (d) *PSNR*= 29.69 dB

Figure 5.23. (a) Original (first frame of QCIF video *Suzie*), reconstructed image using (b) DCT, (c) DWT, (d) Hybrid DWT-DCT

5.4.3 HD videos

In this section, performance analyses of the algorithm on four HD video sequences are presented. Only the first 90 frames of each video are considered since it shows consistent results for all frames. To begin with, 'Stockholm' HD sequence is considered for the analysis. Figure 5.24 shows the *PSNR* for constant *CR* of 96 % for 'Stockholm' sequence. It is clear that proposed hybrid scheme shows the best performance. In Figure 5.25, comparing the three algorithms, it is observed that the hybrid approach is equally effective in HD video as it has the highest compression ratio at constant *PSNR* of 25 dB.

In addition, the algorithm is further verified by using four individual high definition video sequences. All four video sequences: 'Stockholm', 'Shields', 'Ice', and 'City' are obtained from [52]. Individual video sequences are of different nature. For example, the 'Stockholm' video sequence is the panning view over an old town. Similarly the 'City' video sequence is the panning view of a city. In the 'Shield' video sequence, a man is moving his hands over a series of shields. The 'Ice' video sequence shows ice skating with objects in very fast motion.

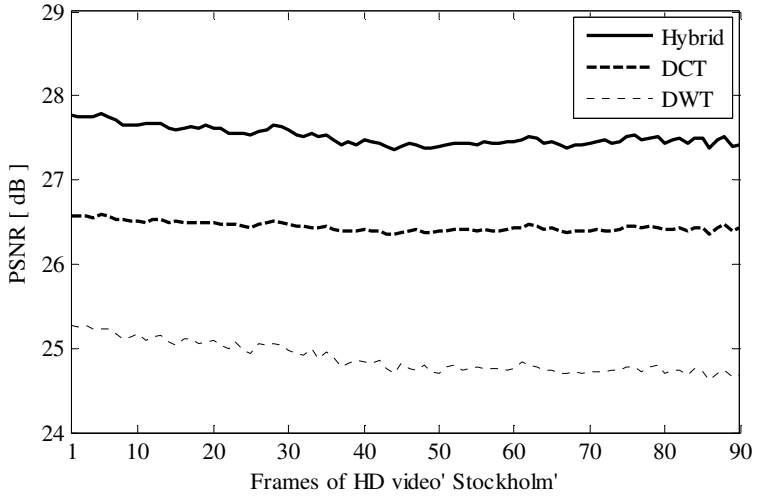

Figure 5.24. *PSNR* for different frames of type 3 video for average compression ratio of 96%

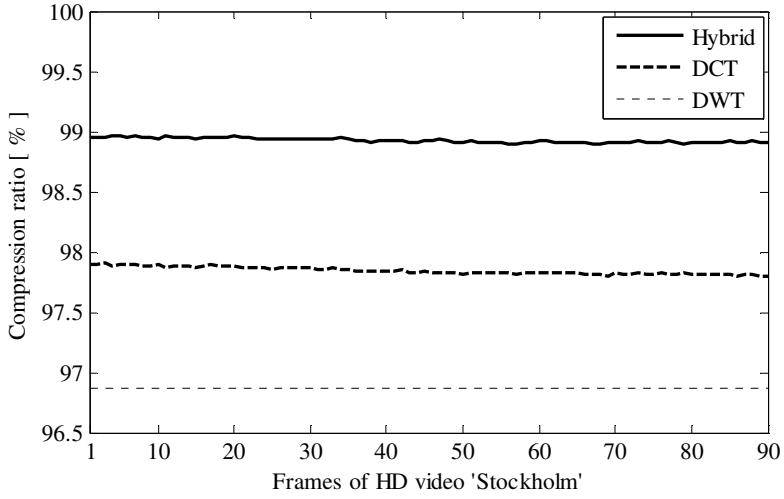

Figure 5.25. Compression ratio for different frames of type 3 video for average *PSNR* of 25 dB

Figure 5.26 represents the average *PSNR* value for four HD videos using proposed hybrid DWT-DCT algorithm, stand alone DCT algorithm and stand alone DWT algorithm for the constant compression ratio of 96 %. It is observed that proposed hybrid algorithm has higher *PSNR* value as compared to other two stand alone algorithms. The deviation of *PSNR* value between proposed hybrid algorithm and DCT is consistent for all kind of video sequences. For video sequence 'Ice', the deviation of *PSNR* value between proposed hybrid algorithm and DWT is higher as compared to the other video sequences. This is due to the fact that video sequence 'Ice' is fast moving as compared to other types of video sequences.

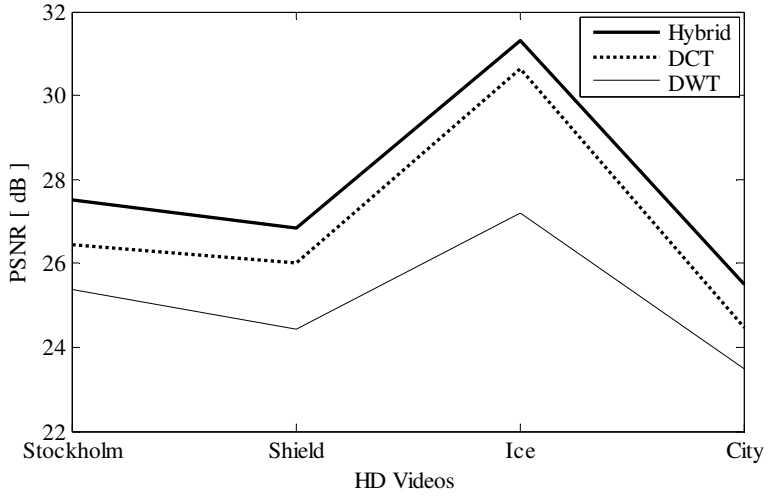

Figure 5.26. Average *PSNR* for 4 different type 3 videos for average compression ratio of 96%

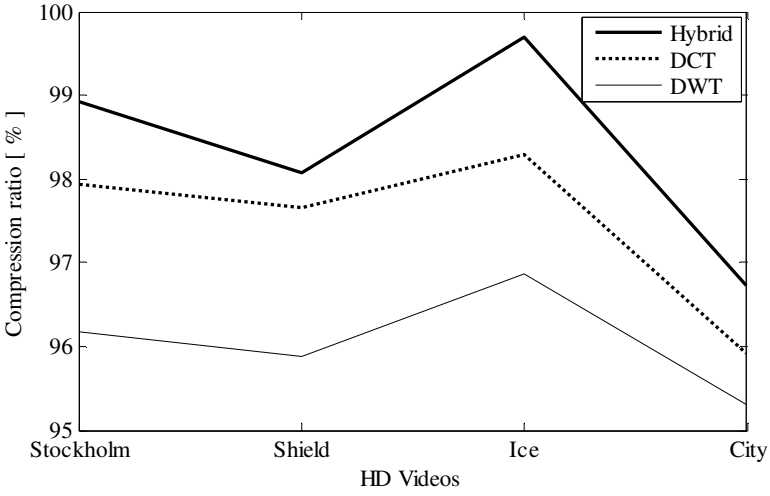

Figure 5.27. Average compression ratio for 4 different type 2 videos for average *PSNR* of 25 dB

From Figure 5.26, it is observed that the average PSNR for the type 2 videos are around 25 dB. Hence for the compression ratio comparison is analyzed at constant PSNR of 25 dB. Figure 5.27 present the compression ratio performance of three algorithms for the HD sequences for constant average *PSNR* of 25 dB. Once again it is seen that proposed hybrid algorithm can be compressed more than that of DWT and DCT to achieve same *PSNR* value. It is also depicted that the hybrid algorithm has better performance for a sequence having fast moving objects like the 'Ice' sequence.

Figure 5.28 shows the analysis of the *SSIM* index for 90 frames of the 'Stockholm' sequence for an average *CR* of 96%. From Fig. 36, it is clear that the *SSIM* index for the DWT algorithm is very low in the range of 0.35, whereas the index value is notably higher for the hybrid algorithm (in the range of 0.65). Note that, the initial *SSIM* is near to unity because the video consists of some black frames.

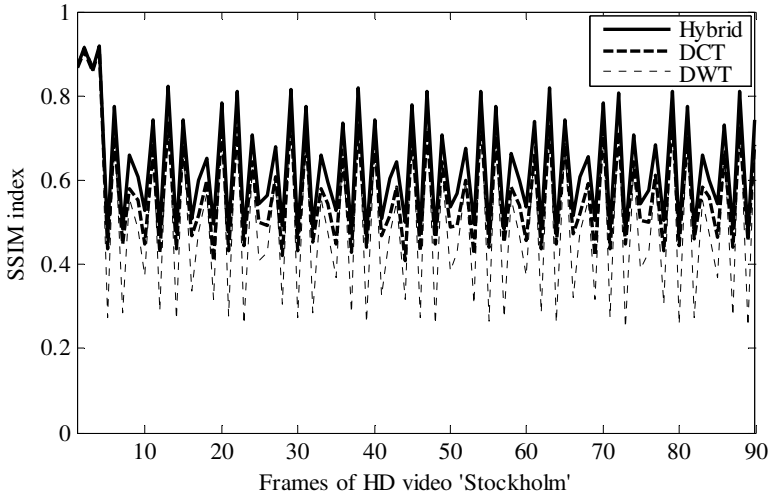

Figure 5.28. *SSIM* index for different frames of type 3 video for average *CR* of 96 %

Figure 5.29 shows the first frame of 'Stockholm' sequence (in grey scale) along with other reconstructed frames using DCT, DWT and proposed hybrid schemes. The *PSNR* using DCT, DWT and proposed hybrid algorithm are 28.94 dB, 27.66 dB, and 29.85 dB, respectively. The DWT algorithm has the lowest PSNR value and the reconstructed image quality of this algorithm also contains noises. The false contouring effect due to extreme compression (i.e., 96%) is clearly visible in the frame reconstructed using the JPEG-based DCT, though its *PSNR* is similar to other schemes. On the other hand, it is clearly visible that the proposed hybrid algorithm is free from the false contouring effects and also has better reconstruction quality as compared to other stand alone algorithms.

(a)Original first frame

(b)*PSNR* = 28.94 dB

(c)*PSNR* = 27.66 dB

(d)*PSNR* = 29.85 dB

Figure 5.29. (a) Original (first frame of HD video *Stockholm*), reconstructed image using (b) DCT, (c) DWT, (d) Hybrid DWT-DCT

5.5 Performance evaluation: Markov Sequence

Finally, the algorithm is tested for first order Markov sequence explained in 4.2III. . All the three algorithms are analyzed to compute the energy compaction property. Figure 5.30 shows the distribution of variances of the transform coefficients for three different transforms. The variances are in decreasing order. In this plot, the *CR* for the DCT, the DWT and the hybrid schemes have been set to 50%, 53% and 50% respectively. It can be seen that, for a given *CR*, the hybrid scheme has the lowest variance distribution, which leads to higher energy compaction property, which in turn leads to higher *PSNR* compared to the other two schemes, as evident in other plots. In other words, for a fixed level of distortion, the number of bits required transmitting the hybrid transformed coefficients would be less than those required for other schemes.

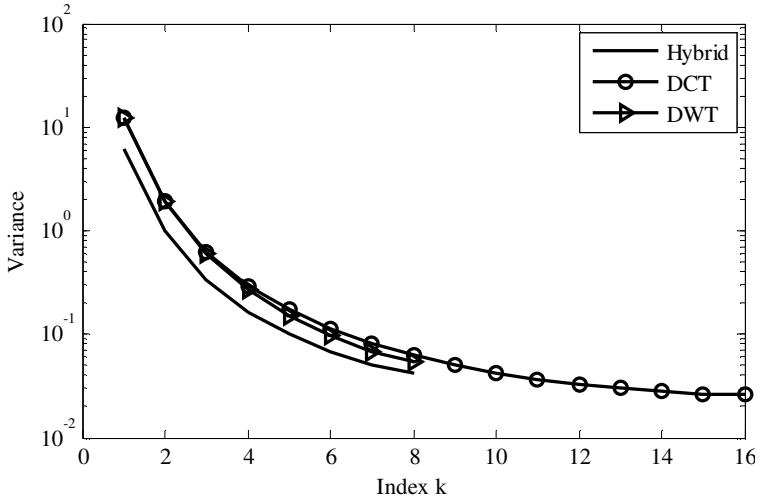

Figure 5.30. Variance distribution of the transform coefficients

5.6 Comparison of results with the recent literatures:

To show the effectiveness of the proposed hybrid DWT DCT algorithm, the algorithm has been compared with some standards: JPEG, JPEG 2000, EZBC, SPIHT, EZW, SPECK and already developed algorithms (Singh et al.) [20], (Yu & Mitra) [19], (HS-HIC) [17], (OB-HIC) [18].

Table 5.3 shows the resulting *PSNR* at bits per pixel (bpp) of 0.25 (*CR*=32%), for standard images: Lena, Barbara and Goldhill using different standards and already developed algorithms: (Yu & Mitra) [19], (HS-HIC) [17], and (OB-HIC) [18].

Table 5.3. Result comparison with recent algorithm

Test images		Lena	Barbara	Goldhill
CR = 32 % (BPP = 0.25)	HS-HIC [17]	35.092	26.13	30.57
	Yu & Mitra [19]	35.0035	31.5928	32.9558
	JPEG	32.49	27.77	29.78
	JPEG2000	34.15	28.89	30.53
	EZBC	34.35	28.25	30.74
	SPECK	34.03	27.76	30.5
	EZW	33.17	26.77	30.31
	SPHIT	34.14	28.13	30.56
	OB-HIC [18]	35.9591	32.8148	33.898
	Proposed	**36.9872**	**31.46**	**35.88**

From the Table 5.3, it is clearly observed that for the standard image 'Lena', and 'Goldhill', the proposed hybrid algorithm performance is better than the performance of other standards and algorithms. For the standard image 'Barbara', the result is comparable to other algorithm. Although the *PSNR* value is comparatively less than other algorithm for this image, the reconstruction quality of proposed algorithm is visually better as compared to other. Figure 5.31, and Figure 5.32 shows the visual illustration of the original and reconstructed image using proposed hybrid algorithm and (OB-HIC) [18] at compression ratio of 64% (bpp=0.125).

(a) Original Image (b) 34.01dB (c) 30.08dB

Figure 5.31. Quality comparison at *CR* of 64% (a) Original image[1], (b) OB-HIC [18] (c) Proposed

[1]Internet: http://sipi.usc.edu/database/index.html



(a) Original image (b) 31.63dB (c) 29.11dB

Figure 5.32. Quality comparison at *CR* of 64% (a) Original image[2], (b) OB-HIC [18] (c) Proposed

From the above Figure 5.31, and Figure 5.32, it is clear that, the reconstructed image of both 'Lena' and 'Barbara' using (OB-HIC) [18] consists of the some blocking artifacts. In contrast, the proposed hybrid algorithm is free from the blocking artifacts even having the less *PSNR* (3.93 dB in Lena, 2.52 for Barbara).

Similarly, Figure 5.33 shows the original and reconstructed image using proposed hybrid algorithm and (HS-HIC) [17] for standard image 'Barbara'. The image is compressed at 32.58 % (bpp = 0.2455). The *PSNR* for reconstructed image Barbara' are 26.13 dB and 29.62 dB using (HS-HIC) [17] and proposed hybrid algorithm, respectively. It is clearly observed that the reconstruction quality is better for proposed algorithm as compared to (HS-HIC) [17].



(a) original image (b)26.13dB (c) 35.88dB

Figure 5.33. Quality comparison at *CR* of 32.58% (a) Original image, (b) HS-HIC [17] (c) Proposed

[2]Internet: http://sipi.usc.edu/database/index.html

Furthermore, the performance of proposed algorithm is also compared with (Yu & Mitra) [19]. Since the authors have considered the standard image 'Airplane', the performance is evaluated for the standard image 'Airplane' at two different compression levels: bpp= 0.151 (*CR* = 52.3801%), and bpp = 0.247 (*CR* = 32.38%). The result is shown in the Table 5.4. It is clearly observed from the table that, proposed hybrid algorithm performs better than (Yu & Mitra) [19].

Table 5.4. Result comparison with (Yu & Mitra)

Algorithm / bpp	(Yu & Mitra)[19] *PSNR*(dB)	**Proposed algorithm *PSNR*(dB)**
0.151	28.15	**31.82**
0.247	30.43	**37.12**

In addition, the proposed algorithm is also compared with the (Singh et al.) [57]. The authors have analyzed various medical images: CT, US, and X-ray images. The proposed algorithm is compared with [57] at various compression level as shown in Table 5.5.

Table 5.5. Result comparison with (Sing et al.)

Image types	bpp	*PSNR* (dB)	
		Singh et al. [57]	**Proposed**
CT images	0.234	34.64	**35.67**
	0.254	34.04	**55.96**
	0.273	32.59	**42.11**
	0.306	32.28	**44.01**
	0.356	31.13	**32.83**
US images	0.179	31.24	**31.37**
	0.204	31.42	**32.72**
	0.24	31.02	**36.56**
	0.312	30.38	**32.67**
	0.482	28.12	**29.76**
X-ray images	0.174	35.00	**44.76**
	0.187	34.91	**36.00**
	0.204	37.13	**40.71**
	0.225	34.41	**57.81**
	0.245	33.23	**47.63**

It is be observed from Table 5.5 that for CT and US images, gain in *PSNR* using the proposed hybrid algorithm is better than the method proposed on [57]. For X-ray images, the proposed method has substantial gain in *PSNR* compared to [57], indicating usefulness of the algorithm. The visual illustrations of one image from each image types are presented in Figure 5.34, Figure 5.35, and Figure 5.36 respectively.

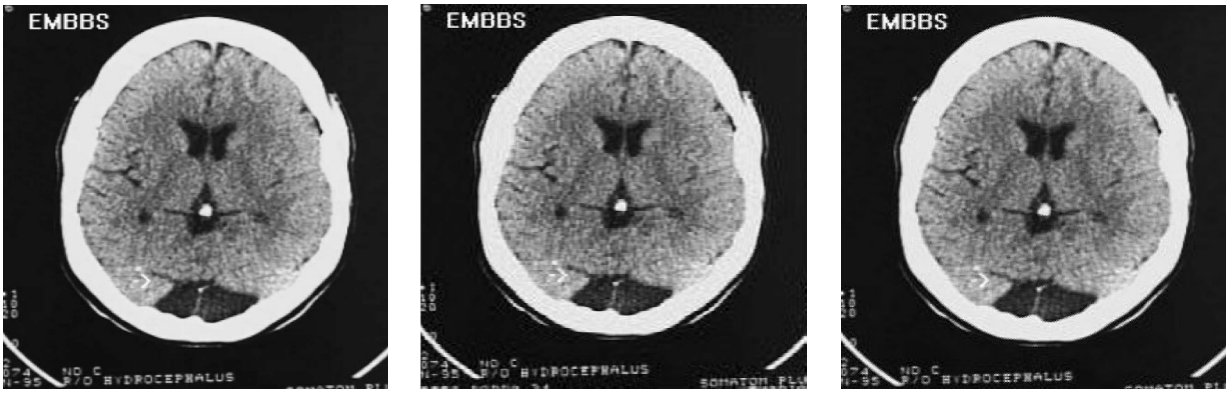

(a) original CT image (b) 31.13dB (c) 32.83dB

Figure 5.34. Quality comparison at *CR* of 22.47% (a) Original image, (b) Singh et al. [57] (c) Proposed algorithm

(a) original US image (b) 28.12dB (c) 29.76dB

Figure 5.35. Quality comparison at *CR* of 16.59% (a) Original image, (b) Singh et al.[57] (c) Proposed algorithm

(a) original X-ray image (b) 34.41dB (c) 57.81dB

Figure 5.36. Quality comparison at *CR* of 34.41% (a) Original image, (b) Singh et al.[57], and (c) Proposed algorithm.

5.7 Summary

Based on the exhaustive simulation results presented above for images and video sequences, it can be seen that the proposed hybrid DWT-DCT algorithm outperforms the JPEG-based DCT, WHT, and the Daubechies-based DWT algorithms. Especially, the hybrid algorithm performs better for the images that consist of detailed view, bright colours, and gradients. Hence, it can be implemented for compressing natural and medical images. The hybrid scheme can also be used for the video sequences consisting of fast moving objects. It is observed that in case of the DWT algorithm, the reconstructed images (and video frames) seem to be the worst, whereas for the DCT, it is affected by artifacts and false contouring effects. However, for the same *CR*, the proposed hybrid algorithm consistently has higher *PSNR* and better reconstruction quality. It is also able to reduce the false contouring effect and artifacts for both images and video frames as illustrated.

CHAPTER 6
CONCLUSION AND FUTURE WORK

6.1 Conclusion

In this research work, a hybrid scheme combing the DWT and the DCT algorithms under high compression ratio constraint for image and video compression has been presented. The algorithm was tested on several types of images, such as, natural, medical, and benchmark images. It was also tested on several types of video sequences, such as, endoscopic, QCIF, and HD videos.

The results of the exhaustive simulations show consistent improved performance for the hybrid scheme compared to the JPEG-based DCT, WHT, and the Daubechies-based DWT schemes. The new scheme has also reduced the false contouring effects and blocking artifacts significantly which occurs in the images reconstructed using DCT algorithm at higher compression ratio. The analysis also showed that for a fixed level of *PSNR*, the number of bits required to transmit the hybrid coefficients would be less than those required for other schemes.

In addition, the energy compaction property of the algorithm was studied using variance analysis in a first order Markov sequence. It was observed that the proposed algorithm has better performance as compared to the other stand alone algorithms.

Moreover, the proposed algorithm was also compared with some standards and already developed hybrid algorithms. It was observed that the proposed hybrid algorithm performs better than the existing algorithms. The proposed scheme is intended to be used as the image/video compressor engine in imaging and video applications where high compression is required.

6.2 Future Work

Going deeper, the result in this thesis provides a strong foundation for future work for the hardware design. Following the results and analysis described in this thesis, a number of future works could be taken up as follows.

I. All of the analysis presented in this thesis work involved exhaustive simulations. The algorithm can be realized in hardware implementation as a future work.

II. The proposed algorithm can also be a good option for the image processor of the wireless capsule endoscopic system.

III. The research work has been analysed for high compression ratio. Further research can be performed to relax high compression ratio constraint.

IV. This work has been constrained only for the removal of the spatial redundancy by compression of still images. Further work can be used for the removal redundancy of the video sequences using inter coding.

REFERENCES

[1] P. N. Topiwala, *Wavelet image and video compression*. Kluwer Academic, 1998.

[2] B. Furht, Ed., *Encyclopedia of Multimedia*. Springer, 2006.

[3] R. K. Rao and P. Yip, *Discrete Cosine Transform: Algorithms, Advantages and Applications*. NY: Academic, 1990.

[4] W. B. Pennebaker and J. L. Mitchell, *JPEG Still Image Data Compression Standard*, 3rd ed. New York: Springer, 1993.

[5] G. Joy and Z. Xiang, "Reducing false contours in quantized color images," *Computer and Graphics, Elsevier*, vol. 20, no. 2, pp. 231–242, 1996.

[6] L. Chen, *VLSI Design of Wavelet Transform: Analysis, Architecture and Design Examples*. Imp. College press, 2007.

[7] R. A. DeVore, B. Jawerth, and B. J. Lucier, "Image compression through wavelet transform coding," *IEEE Transactions on Information Theory*, vol. 38, no. 2, pp. 719–746, 1992.

[8] G. Strang and T. Nguyen, *Wavelets and Filter Banks*. Cambridge Press, 1996.

[9] J. M. Shapiro, "Embedded image coding using zerotrees of wavelet coefficients," *IEEE Transactions on Signal Processing*, vol. 41, no. 12, pp. 3445–3462, 1993.

[10] A. Said and W. A. Pearlman, "A new, fast, and efficient image codec based on set partitioning in hierarchical trees," *IEEE Transactions on Circuits and Systems for Video Technology*, vol. 6, no. 3, pp. 243–250, 1996.

[11] ISO/IECJTCI/SC29/WG1 N871 R, "Embedded, independent block-based coding of subband data," July 1998.

[12] ISO/IECJTCI/SC29/WG1 N1020 R, "EBCOT: Embedded block coding with optimized truncation," Oct. 1998.

[13] A. Said and W. Pearlman, "Low-complexity waveform coding via alphabet and sample-set partitioning in visual communications and image processing," in *Proc. SPIE*, 1997, pp. 25–37.

[14] S.-T. Hsiang and J. W. Woods, "Embedded image coding using zeroblocks of subband/wavelet coefficients and context modeling," in *Proc. ISCAS 2000 Geneva Circuits and Systems*, vol. 3, 2000, pp. 662–665.

[15] R.Costantini, J.Bracamonte, G.Ramponi, J.L.Nagel, M.Ansorge, and F.Pellandini, "Low complexity video coder based on discrete Walsh Hadamard transform," in *Proc. European signal processing conference*, 2002, pp. 1217–1220.

[16] M. Ezhilarasan and P. Thambidurai, "A hybrid transform technique for video coding," *LNCS*, vol. 4308, pp. 503–508, 2006.

[17] U. S. Mohammed, "Highly scalable hybrid image coding scheme," *Digital Signal Processing,Science Direct*, vol. 18, pp. 364–374, 2008.

[18] U. S. Mohammed and W. M. Abd-elhafiez, "Image coding scheme based on object extraction and hybrid transformation technique," *Int. J. of Engineering Science and Technology*, vol. 2, no. 5, pp. 1375–1383, 2010.

[19] T.-H. Yu and S. K. Mitra, "Wavelet based hybrid image coding scheme," in *Proc. IEEE Int Circuits and Systems Symp*, vol. 1, 1997, pp. 377–380.

[20] R. Singh, V. Kumar, and H. K. Verma, "DWT-DCT hybrid scheme for medical image compression," *Medical Engineering and Technology*, vol. 31, pp. 109–122, 2007.

[21] F. Zhijun, Z. Yuanhua, and Z. Daowen, "A scalable video coding algorithm based DCT-DWT," in *Proc. 3rd IEEE Int. Symp. Signal Processing and Information Technology*, 2003, pp. 247–249.

[22] P. J. Paul and P. N. Girija, "A novel VLSI architecture for image compression," in *Proc. ISM'06 Multimedia Eighth IEEE Int. Symp*, 2006, pp. 794–795.

[23] K. A. Wahid, M. A. Islam, S. S. Shimu, M. H. Lee, and S. Ko, "Hybrid architecture and VLSI implementation of the Cosine-Fourier-Haar transforms," *Circuits, Systems, and Signal Processing*, vol. 29, no. 6, pp. 1193–1205, 2010.

[24] S. Jiang and X. Hao, "Hybrid Fourier-Wavelet image denoising," *Electronics Letters*, vol. 43, no. 20, pp. 1081–1082, 2007.

[25] A. H. Ali, "Combined DWT-DCT digital image water marking," *Computer science*, vol. 3, no. 9, pp. 740–746, 2007.

[26] H. Qi, Q. Huang, and W. Gao, "A low-cost very large scale integration architecture for multistandard inverse transform," *IEEE Transactions on Circuits and Systems II: Express Briefs*, vol. 57, no. 7, pp. 551–555, 2010.

[27] C. Fan and G. Su, "Fast algorithm and low-cost hardware-sharing design of multiple integer transforms for VC-1," *IEEE Transactions on Circuits and Systems II: Express Briefs*, vol. 56, no. 10, pp. 788–792, 2009.

[28] C. P. Fan and G. A. Su, "Efficient fast 1-d 8 × 8 inverse integer transform for VC-1 application," *IEEE Transactions on Circuits and Systems for Video Technology*, vol. 19, no. 4, pp. 1–7, 2009.

[29] K. Wahid, S.-B. Ko, and D. Teng, "Efficient hardware implementation of an image compressor for wireless capsule endoscopy applications," in *Proc. IEEE Int. Joint Conf. Neural Networks*, 2008, pp. 2761–2765.

[30] A. Rosenfeld and A. C. Kak, *Digital picture processing*. Academic Press Inc., 1982.

[31] N. C. Giri, *Multivariate statistical inferences*. Academic Press Inc., 1977.

[32] D. Salomon, *Data compression: the complete reference*, 2nd ed. New York: Springer, 2000.

[33] N. Ahmed, T. Natarajan, and K. Rao, "Discrete Cosine Transfom," *Computers, IEEE Transactions on*, vol. C-23, no. 1, pp. 90 – 93, Jan 1974.

[34] V. Bhaskaran and K. Konstantinides, *Image and Video Compression Standards: Algorithm and Architectures*, 2nd ed. Kulewer Academic Publisher, 1997.

[35] K. R. Rao and P. Yip, *Discrete Cosine Transform: Algorithms, Advantages, Applications*. Boston: Academic Press, 1990.

[36] J. D. Kornblum, "Using JPEG quantization tables to identify imagery processed by software," *Digital Forensic Workshop, Elsevier*, pp. 21–25, 2008.

[37] I. Daubechies, *Ten Lectures on Wavelets*. SIAM, 1992.

[38] S. G. Mallat, "A theory for multiresolution signal decomposition: the wavelet representation," *IEEE Transactions on Pattern Analysis and Machine Intelligence*, vol. 11, no. 7, pp. 674–693, 1989.

[39] H. C. Andrews and J. Kane, "Kronecker matrices, computer implementation, and generalized spectra," *JACM*, vol. 17, no. 2, pp. 260–268, April 1970.

[40] H. C. Andrews and K. L. Caspari, "A generalized technique for spectral analysis," *IEEE Transactions on Computers*, no. 1, pp. 16–25, 1970.

[41] S. Shrestha and K. Wahid, "Hybrid DWT-DCT algorithm for biomedical image and video compression applications," in *Proc. IEEE International Conference on Information Sciences, Signal Processing and Applications*, 2010, pp. 280–283.

[42] S. E. Ghrare, M. A. M. Ali, M. Ismail, and K. Jumari, "Diagnostic quality of compressed medical images: Objective and subjective evaluation," in *Proc. Second Asia Int. Conf. Modeling & Simulation AICMS 08*, 2008, pp. 923–927.

[43] D. S. Hands, Q. Huynh-Thu, A. W. Rix, A. G. Davis, and R. M. Voelcker, "Objective perceptual quality measurement of 3g video services," in *Proc. Fifth IEE Int. Conf. 3G Mobile Communication Technologies 3G 2004*, 2004, pp. 437–441.

[44] H. S. Z. Wang, A. Bovik and E. Simoncelli, "Image quality assessment: From error measurement to structural similarity," *IEEE Trans. Image Processing*, vol. 13, no. 4, pp. 600–612, 2004.

[45] R. W. R. Gonzalez and S. Eddins, *Digital Image Processing using MATLAB*. Pearson Prentice Hall, 2004.

[46] N. Ahmed and K. R. Rao, *Orthogonal Transforms for Digital Signal Processing*. Springer, 1975.

[47] A. K. Jain, *Fundamentals of Digital Image Processing*. Prentice Hall Inc., 1989.

[48] Z. Wang and A. C. Bovik, "Mean squared error: Love it or leave it? a new look at signal fidelity measures," *IEEE Signal Processing Magazine*, vol. 26, no. 1, pp. 98–117, 2009.

[49] "Gastrolab-the gastrointestinal site," Aug 28 2010. [Online]. Available: www.gastrolab.net

[50] "The USC-SIPI image database," Aug 25 2010. [Online]. Available: http://sipi.usc.edu/-database/index.html

[51] D. O. Faigel and D. R. Cave, *Capsule endoscopy*. Elsivier, 2008.

[52] "Network Systems Lab," Aug 8 2010. [Online]. Available: http://nsl.cs.sfu.ca/wiki/-index.php/Video_Library_and_Tools#Video_Tools

[53] N. Thomos, N. V. Boulgouris, and M. G. Strintzis, "Optimized transmission of JPEG2000 streams over wireless channels," *IEEE Transactions on Image Processing*, vol. 15, no. 1, pp. 54–67, 2006.

[54] X. Li and J. Cai, "Robust transmission of JPEG2000 encoded images over packet loss channels," in *Proc. IEEE Int Multimedia and Expo Conf*, 2007, pp. 947–950.

[55] H. N. K. A. Saffor, A. R. Ramil and D. Dowsett, "Objective and subjective evaluation of compressed computed tomography images," *Internet Journal of Radiology*, vol. 2, no. 2, 2002.

[56] S. Garawi, R. S. H. Istepanian, and M. A. Abu-Rgheff, "3 G wireless communications for mobile robotic tele-ultrasonography systems," *IEEE Communications Magazine*, vol. 44, no. 4, pp. 91–96, 2006.

[57] S. Singh, V. Kumar, and H. K. Verma, "DWT-DCT hybrid scheme for medical image compression." *J Med Eng Technol*, vol. 31, no. 2, pp. 109–122, 2007.

APPENDIX

SAMPLE IMAGES USED FOR PERFORMANCE ANALYSIS

A.1 Sample Natural Images (1024 × 1024) captured by Nikon D40 X DSLR Camera

1

2

3

4

5

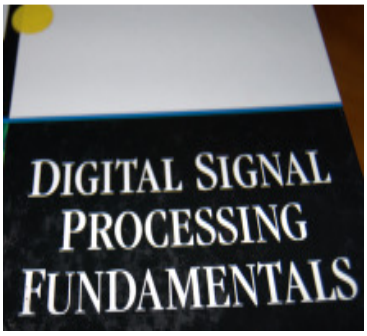

6

7

8
(1526 × 1020)

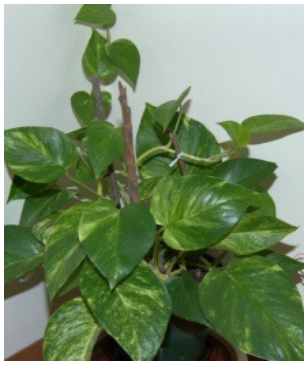

9
(1526 × 1020)

10
(1526 × 1020)

A.2 Sample Medical Images (256 × 256) obtained from [49]

1

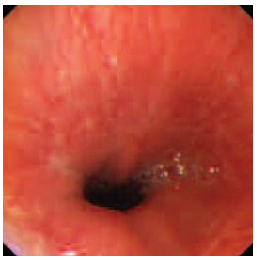

2

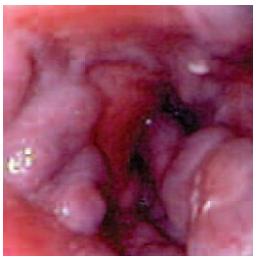

3

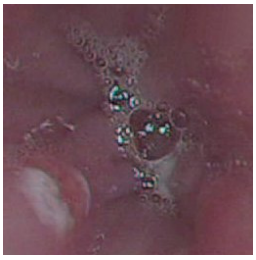

4

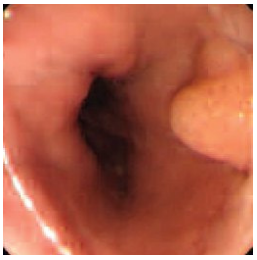

5

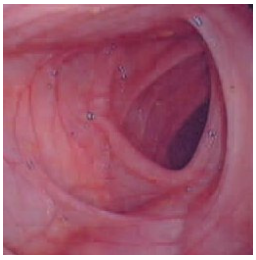

6

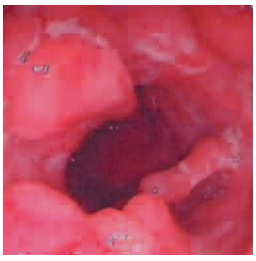

7

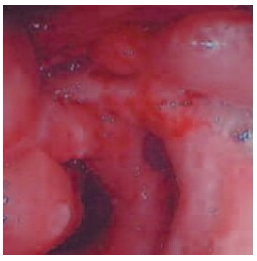

8

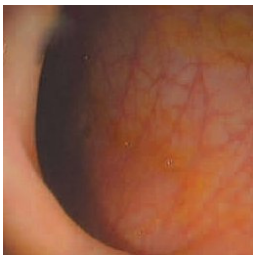

9

10

11

12

13

14

15

16

A.3 Sample Benchmark Images (256×256) obtained from [50]

1

2

3

4

5